MINISTERIO DE DEFENSA

REAL INSTITUTO Y OBSERVATORIO DE LA ARMADA
EN SAN FERNANDO

**BOLETIN ROA**
**No. 3/2005**

# Study of Seismic Noise Recorded at the Broadband Station MELI in the Year 2000

ANDREAS FICHTNER

Foto Portada:
Fachada Edificio Principal del Real Instituto y Observatorio de la Armada.
(Siglo XVIII).

MINISTERIO DE DEFENSA

REAL INSTITUTO Y OBSERVATORIO DE LA ARMADA
EN SAN FERNANDO

**BOLETIN ROA**
**No. 3/2005**

# Study of Seismic Noise Recorded at the Broadband Station MELI in the Year 2000

ANDREAS FICHTNER

Edita:

MINISTERIO
DE DEFENSA

SECRETARIA
GENERAL
TECNICA

Imprime: Real Instituto y Observatorio de la Armada
San Fernando (Cádiz). Febrero 2005
Depósito Legal: CA 469-78
ISSN 1131-5040
NIPO 076-05-032-9

# Study of Seismic Noise

# Recorded at the Broadband Station

# MELI in the Year 2000

ANDREAS FICHTNER

**Acknowledgements**

This work has been carried out at the *Royal Naval Institute and Observatory (Real Instituto y Observatorio de la Armada, ROA) of the Spanish Navy* in San Fernando, Spain, during the month of September 2003 and at the *Department of Earth and Space Sciences* at the *University of Washington* in Seattle, USA, between March and July 2003. It was made possible through the help of countless people who provided the technical resources and shared their intellectual ones.

All the data were provided by the *Royal Naval Institute and Observatory*. The very labor-intensive work of reading the tapes was done by Guillermo Muñoz-Delagdo Serrano and Jesús Quijano Junquera. Thank you so much!

I am greatly indebted to Simone Cesca and Professor Elisa Buforn at the *Universidad Complutense* in Madrid, for their inspiration and advice, for fruitful discussions and for almost instantaneously answering numerous e-mails.

José Martín Dávila, Jesús Quijano Junquera, Guillermo Muñoz-Delagdo Serrano, José Prian Nieto and José Antonio Peña García helped me whenever I encountered a problem and gave me continuous support.

Most of all, I want to thank Antonio Pazos for keeping in contact with me via e-mail for almost one year and for being available whenever I needed help. Without his willingness to share his knowledge and experience, and without being patient when it took me a little longer to understand, this study would not have been possible.

Finally, it is my pleasure to thank all those who work at the *Royal Naval Institute and Observatory* for their friendship and for making my stay an unforgettable academic and cultural experience.

This work was supported by the *Ministerio Español de Ciencia y Tecnología* as part of the research project TEDESE: REN 2000-0777-C02-02 RIES, and ERSE: REN 2003-05178-C03-02.

**Table of Contents**



**NOTE: A PDF file with figures in color is placed in the back cover.**

## 1. Introduction

Seismic noise studies for permanent broadband stations have become a standard in recent years. An exact knowledge of noise amplitudes and frequency content provides an objective measure of station quality, information about geologic structures (PAROLAI et al., 2002), human activity and the influence of climate phenomena on the solid Earth.

The list of factors contributing to seismic noise is practically interminable. It includes all kinds of human activity, atmospheric pressure variations, surface temperature variations (GORDEEV et al., 1992), wind (TANIMOTO, 1999, and WILCOCK et al., 1999), ocean waves, Earth tides and seismic waves (PRIVALOVSKIY AND BERESNEV, 1994)

Since each source of seismic noise has its characteristic frequency content, noise can be studied most effectively by considering its power spectral density instead of analyzing displacement, velocity or acceleration seismograms.

Seismic noise can be modelled as a stationary stochastic process without a defined phase spectrum (Bormann, 2002), so the FOURIER integral does not converge and consequently, amplitude spectral density and phase spectrum can not be calculated. Instead, we introduce the power spectral density as the Fourier transform of the *autocorrelation function* $P(\tau)$ of the seismic noise signal f(t).

$$P(\tau) = \langle f(t) \cdot f(t + \tau) \rangle ,$$

where the symbol $\langle . \rangle$ represents the average over a time interval. The *power spectral density* $P(\omega)$ is then given by

$$P(\omega) = F[P(t)] = \int P(\tau) e^{i\omega\tau} \, d\tau .$$

Power spectral densities provide the most appropriate mathematical characterization of seismic noise (AKI and RICHARDS, 2002). Note that if we consider acceleration seismograms with units of $m \cdot s^{-2}$ the units of the corresponding power spectral densities are $m^{-2} \cdot s^{-4} \cdot Hz^{-1}$. They are commonly expressed in dB referenced to 1 $m^{-2} \cdot s^{-4} \cdot Hz^{-1}$.

In order to objectively evaluate a given power spectral density (PSD), reference curves have been elaborated by PETERSON (1993). These curves, called the *New Low-Noise Model (NLNM) and New High-Noise Model (NHNM)* define upper and lower limits of power spectral density at given frequencies. They represent the currently accepted standard for the upper and lower bounds of seismic noise PSD's. Power spectral densities exceeding the NHNM curve indicate an unfavorable station location, whereas power spectral densities below the NLNM curve indicate an erroneous instrument calibration.

One of the main goals of seismic noise studies is the comparison with results from other stations. Hence, it is necessary that all studies follow a given scheme in order to guarantee comparability. Such a scheme has been established by IRIS (1993b) and adapted by CESCA (2001b). It forms the technical basis of this study.

The principal steps can be summarized as follows:

i) Random selection of time windows that do not contain recordings of seismic events for channels BH, LH and VH as well as for all three orientations: North-South (N), East-West (E), vertical (Z).
ii) Estimation of robust power spectral densities.
iii) Correction for the instrument response.
iv) Graphical representation and interpretation.

A detailed description of the more technical aspects is beyond the scope of this study. It can be found in the publications by IRIS (1993b) and CESCA (2001a, 2001b).

## 2. Characteristics of the broadband station MELI

The object of this study is the broadband station MELI (figure 2.1) located in the Autonomous City of Melilla (a Spanish city located Northern Africa). It is one of four stations (MELI, SFUC, CART, MAHO) that currently form the broadband station network ROA/UCM/GFZ (BUFORN et al., 2002). Since its installation, carried out in cooperation between the *Real Instituto y Observatorio de la Armada* (ROA), *the Universidad Complutense de Madrid* (UCM), the *GeoforschungsZentrum Potsdam* (GFZ) and *the Eidgenössische Technische Hochschule in Zürich* (ETH), between 13 and 17 December 1999, the station operates continuously (ROA, 2001). Additional information at www.roa.es or pazos@roa.es.

The technical characteristics of station MELI are:

i) Sensor: STRECKEISEN STS-2 (provided by the ETH in Zürich until November 2001).
ii) Data acquisition system: QUANTERRA, 3 channels, 24 bit resolution.
iii) Time receiver: GPS.
iv) Telephone connection via modem. Using a PC-Seiscomp, the system operates in quasi real time. This makes the data available in real time at ROA which acts as data collection center.

According to international standards MELI has to be classified as *coastal station* because it is located at less than 1 km away from the coast of the Mediterranean Sea. The location is shown in the table 2.1.

| Geographic Information, MELI | |
|---|---|
| **Latitude** | 35.290 North |
| **Longitude** | 2.938 West |
| **Elevation** | 20 m |
| **Distance from coast** | Less than 1 km |

**Table 2.1** - *Geographic coordinates of station MELI.*

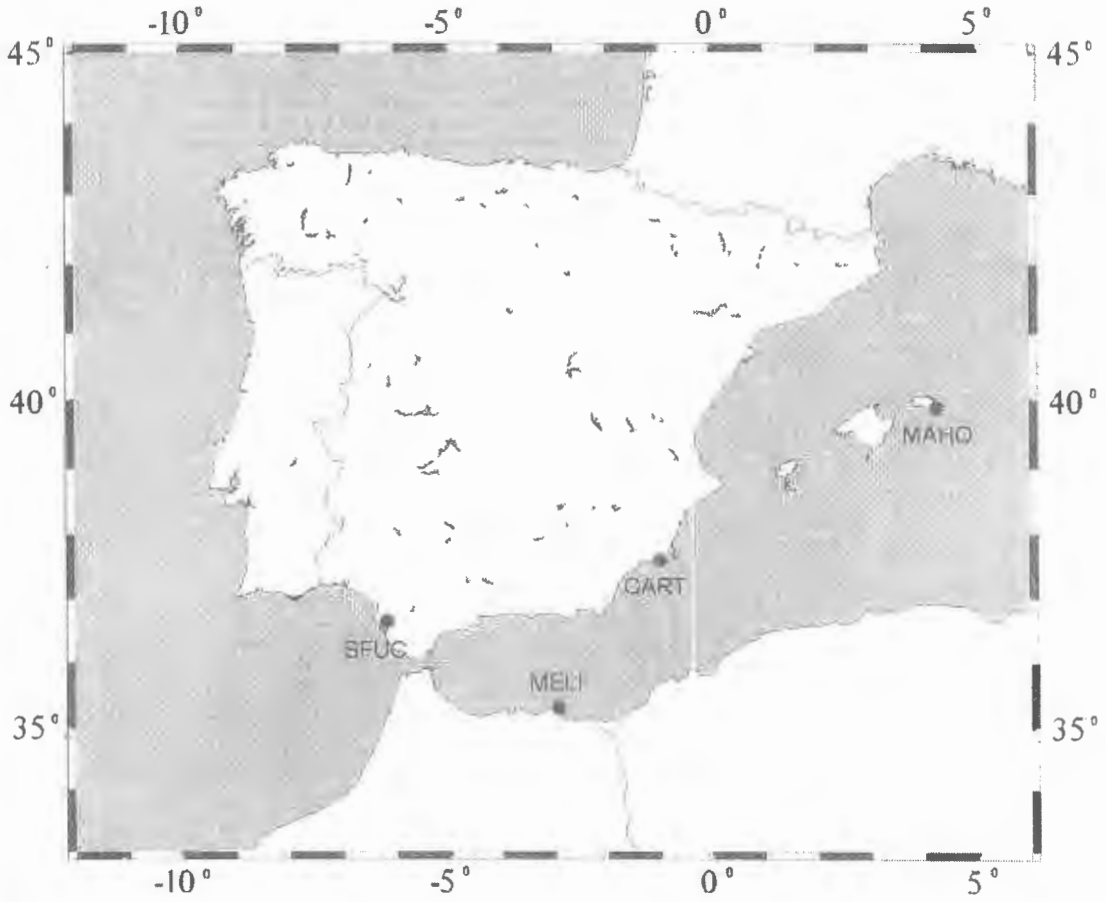


**Figure 2.1** - *Geographic location of broadband stations MELI, SFUC, CART, MAHO (Rubio, 2001).*

The location in an ancient mining viaduct close to the coast and in the middle of a lively Spanish city in North Africa with 67.000 inhabitants is undoubtedly not optimal. However, it is the only possible location in Spain for this region.

In spite of its expected low signal to noise ratio the station is of considerable relevance due to the sparse distribution of stations with these characteristics in Northern Africa. A map of seismic broadband stations in the European-Mediterranean area can be found on the ORFEUS website (http://orfeus.knmi.nl/other.services/network.shtml).

As a consequence of MELI's unique location we can expect to observe interesting phenomena, related for example to human activities that are not observable in places further away from urban centres or the coast.

## 3. Selection of time windows

A seismic noise study requires the random selection of time windows for each channel (BH, LH, VH) and each orientation (N, E, Z) that contain seismic noise and no information related to earthquakes. CESCA (2001a) describes the technical aspects of this selection process in detail. The time windows are chosen randomly from the recordings of one complete year, in this case the year 2000.

The exclusion of time windows containing earthquake data is of considerable importance for noise studies because such data may alter the resulting power spectral densities significantly. Due to tectonic activities in Northern Africa and on the Iberian Peninsula it is important to exclude regional earthquakes as well, even though they have a small magnitude.

In order to study mean PSDs and temporal variations of seismic noise it is important to select approximately the same number of time windows from each season and each day time without favouring a certain temporal interval. An example, for channel BH, is shown in figure 3.1.

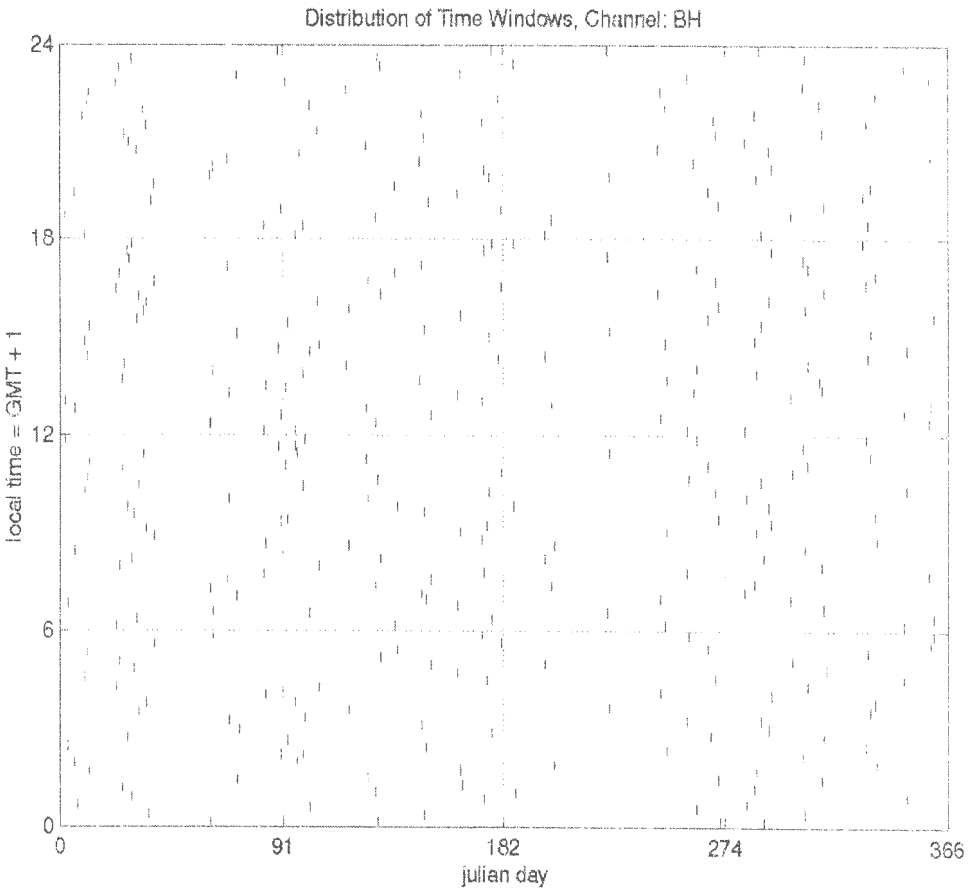


**Figure 3.1** - *The figure shows all time windows (represented by small black lines) for the BH channel used in this study.*

Areas of sparse temporal sampling are on the one hand due to sequences of large global or regional earthquakes that must be excluded from the noise analysis. On the other hand, they are a direct consequence of the random process used for the selection of earthquake-free time windows.

For most of this study we used the time intervals indicated in table 3.1. They have been chosen according to typical periods of human and industrial activity or inactivity and were also used in other studies of seismic noise (CESCA, 2001a, 2001b).

| | January-March (winter) | April-June (spring) | July-September (summer) | October-December (autumn) |
|---|---|---|---|---|
| 0 h – 6 h | The 16 possible combinations of seasonal time intervals (columns) and day time intervals (rows) allow a detailed analysis of temporal variations of the noise PSD. | | | |
| 6 h – 12 h | | | | |
| 12 h – 18 h | | | | |
| 18 h – 24 h | | | | |

**Table 3.1** - *Temporal intervals used in this study.*

By using the mean power spectral density for a whole year as a reference, this choice of time intervals allows us to consider both diurnal and seasonal variations. More details on this can be found in the following sections of this report.

| Channel | Components | Sampling Interval (s) | Period Interval (s) | Number of time windows | Length of time windows (min) |
|---|---|---|---|---|---|
| BH | E, N, Z | 0.05 | 0.25 – 100 | 672 | 6.2 |
| LH | E, N, Z | 1.0 | 8 – 1000 | 25 | 125 |
| VH | E, N, Z | 10.0 | 50 – 10000 | 19 | variable |

**Table 3.2** - *Characteristics of selected time windows. The number of time windows is the number for each of the three components. (The period interval is the inverse of the sampling interval).*

Since each channel is characterized by a different sampling rate (see the table 3.2), the window lengths, in seconds cannot be the same for all three channels. For example, in the case of the channel VH, with a sampling interval of 10 seconds, the time windows have to be significantly longer than those for the BH channel, with a sampling interval of only 0.05 s.

As can be seen in table 3.2, the number of time windows varies significantly from channel to channel, thus allowing different types of studies. Due to technical problems with reading the data tapes, only a relatively small number of time windows for the LH channel were available for this study. Consequently, an analysis of daily variations was possible only for the channel BH and not for the LH and VH channels. Seasonal variations could be studied for all three channels.

## 4. Analysis of seismic noise

As already mentioned, the analysis of seismic noise is based on robust power spectral density estimates. The results are shown in a series of figures (see Appendices A, B, C1 and C2) together with PETERSON'S (1993) noise models.

Also, two vertical lines representing the approximate location of the microseismic peaks expected at periods around 7 s and 14 seconds (Bormann, 2002) are shown.

## 4.1. Complete Year 2000

A calculation of the power spectral density on the basis of all time windows for one complete year gives an overview of the power spectral density as a function of period at a seismic station. The result of this calculation for station MELI is shown in the figure 4.1 and in a larger format in Appendix A. It can be interpreted as the mean power spectral density over the whole year as a function of period.

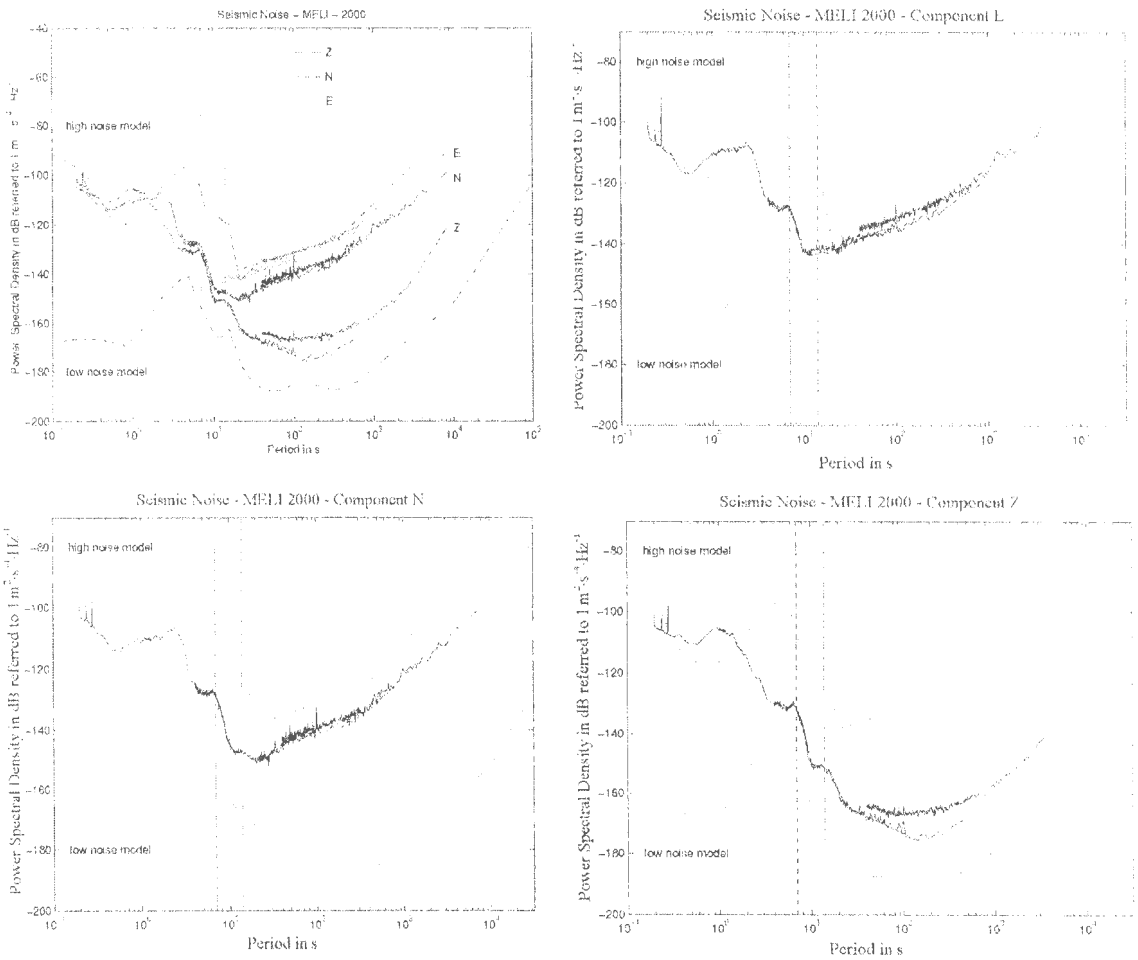


**Figure 4.1** - *Power spectral densities of seismic noise recorded in 2000 at station MELI. The spectrum corresponds to accelerations in* $m \cdot s^{-2}$. *Dash-dotted lines are PETERSON'S noise models (high-noise model and low-noise model). The vertical dotted lines correspond to the 7s and 14s period peaks respectively.* ***Upper left****: Power spectral densities for all channels (BH, LH, VH) and all components (N,E,Z).* ***Upper right****: Power spectral density of all E components.* ***Lower left****: Power spectral densities of all N components.* ***Lower right****: Power spectral densities of all vertical components.*

The noise power spectrum contains a series of interesting aspects that should be pointed out:

1. Throughout the considered frequency band the power spectral densities are closer to PETERSON'S (1993) high-noise model (NHNM) than to the low-noise model (NLNM), the only exception being the vertical component (Z) at periods larger than 10 s. Between periods of approximately 0.2s and 2s the power-spectral densities of all three orientations (Z, N, E) exceed the high-noise model curve by as much as 10 dB or more. Certainly, the most probable explanation for this phenomenon is the

proximity to anthropogenic noise sources such as busy streets, the sea port and the electric power plant which usually generate high-frequency seismic noise (HFSN). More difficult to explain is the significant difference between the PSD's of vertical and horizontal components at low frequencies. Smaller differences have been observed by other authors (CESCA, 2001a). Usually, low-frequency seismic noise (LFSN) is explained by variations in atmospheric conditions such as temperature and pressure.

2. A number of clearly visible peaks can be observed even in the robust power spectral density plots for the BH channel. Three prominent peaks (figure 4.2) are located at periods of 0.20 s, 0.24 s and 0.28 s. All three spatial orientations show this phenomenon but with different peak amplitudes. The analysis of seasonal and daily variations will provide more information about the nature of these peaks. Since they occur at very small periods, only the BH channel can be used to infer a detailed characterization of their properties.

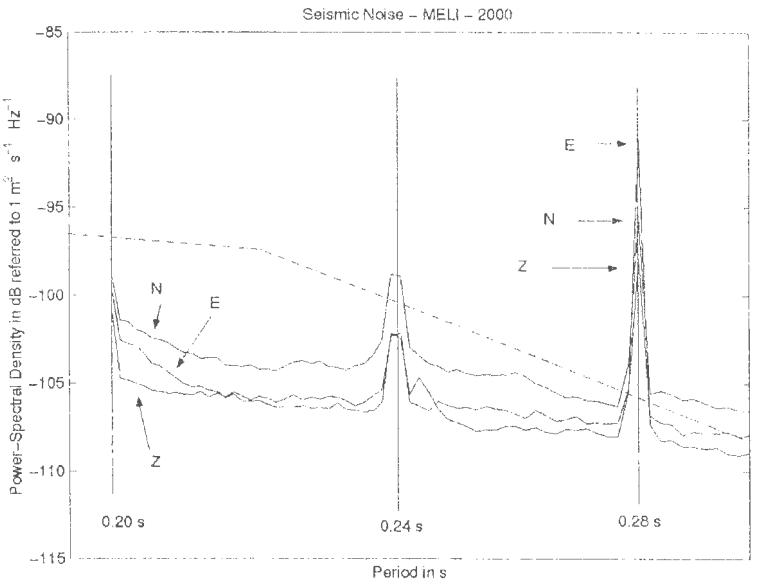


**Figure 4.2** - *Three prominent peaks in power spectral densities at 0.20 s, 0.24 s and 0.28 s for all three orientations*

Another less pronounced peak appears at periods of approximately 100 s (figure 4.3). Interestingly, this peak is clearly discernible only in the PSDs of the horizontal components whereas it is less clearly pronounced in the vertical direction. Furthermore, it is higher for the VH channel than for the LH channel even though data are available for both in the period range from 40 s to 820 s. Probably, the reason for this is the smaller resolution obtained for the LH channel (a smaller number of points per period interval) at large periods compared to the resolution obtained for the channel VH. However, also in this case, only an analysis of temporal variations can provide more information about the character of these peaks

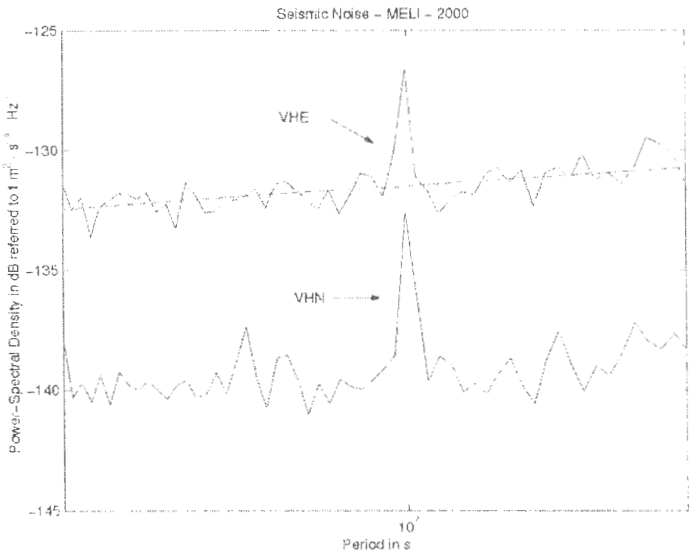


**Figure 4.3** - *Peaks in power spectral density of the horizontal VH channels at the period of 100 s.*

Given the enormous magnitude of the observed peaks it also remains to check if they could be the result of numerical problems.

3. At periods around 1s (figure 4.4) he PSD of the vertical direction is clearly higher than for the two horizontal directions. A considerable drop can be observed at about 1.5 s for the vertical component whereas the two horizontal components show an increasing PSD and a similar drop at 2.7 s.

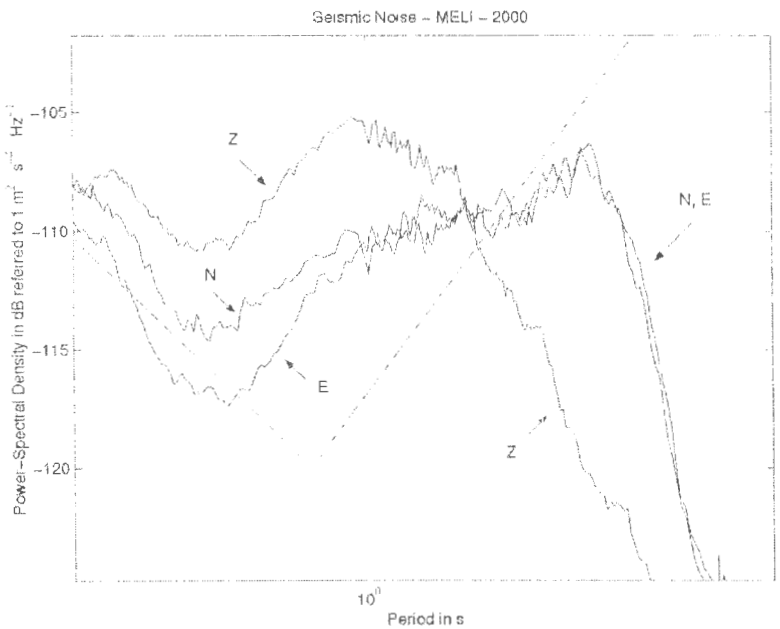


**Figure 4.4** - *Power spectral densities of all three spatial components at periods around 1 s.*

Differences between the PSDs of horizontal and vertical components are a feature that can be observed worldwide. Usually it is attributed to the regional geology and in particular to sedimentary layers. Since seismic noise is thought to be largely composed of LOVE and RAYLEIGH waves, the relative amplitude of LOVE and RAYLEIGH modes at different frequencies can contain geologic information. PAROLAI, BORMANN and MILKEREIT (2002) used the H/V ratio to infer sediment layer thicknesses. However, it is not sufficient to consider only one station in order to develop such regionally varying relationships.

4. The microseismic peaks are identifiable in the power spectral density plot, especially in the vertical direction. Even though the station is very close to the coast, they are not as pronounced as one might expect. In part responsible for this effect may be the high PSD itself, since it could mask these natural peaks with anthropogenic noise. Additionally, the Mediterranean Sea is characterized by a smaller wave activity than the Atlantic Ocean for example. Hence, the microseismic peaks, generated mainly by wave activity, are naturally smaller. Additionally, the peaks do not occur exactly at periods of 7 s and 14 s. This was to be expected because these periods depend strongly on factors such as water depth, wind activity and thus have to be understood as a rough orientation and not as exact values.

   At this point it is especially important to note that the noise models proposed by PETERSON (1993) are mainly based on stations in the Americas, Japan and China. Consequently, the stations are either continental or close to the oceans where wave-generated noise can be expected to be more important than civilizational noise.

5. An interesting feature is the difference between the PSD of channel LH and channel VH in the interval from 40 s to 820 s. Theoretically this difference should not exist. The curves representing different orientations should overlap in the frequency range that the respective channels have in common, as is the case for channels BH and LH. CESCA (2001, a) attributed this difference to the small number of time windows for channel VH which results in a less reliable estimation of power-spectral densities. However, the fact that such a difference does not exist between the PSDs of channels BH and LH (the number of windows for LH is comparable to the number of windows for VH channel, due to technical problems, as we explained before.) suggests that this explanation is unlikely. Later, we will discuss this problem, which is probably of numeric character, more in detail.

6. Especially at high frequencies the power spectral density seems to be displaced toward higher frequencies with respect to PETERSON'S noise models. This blue shift of the noise spectrum might be explained by the proximity of high frequency noise sources. (As we explained before, MELI is located in the city centre.) If a source, for example a street or the sea port, is located very close to the station, seismic wave attenuation plays a smaller role. Hence, higher frequencies are more likely to be recorded. As a consequence the unattenuated noise is characterized by higher frequencies and higher amplitudes. It is not possible to separate both effects.

Evidently, a large number of phenomena can be observed. It is almost impossible to find unique interpretations for all or even a majority of them. Seismic noise contains an enormous amount of information. Numerous contributions are of comparable

importance and many of them have similar characteristics. Consequently, a separation and identification of contributing effects is extremely difficult. An analysis of temporal variations of seismic noise can help to increase the understanding of some observations.

## 4.2. Seasonal Variations

Prior to a detailed analysis of temporal variations it is important to explain the strategy used for this type of study.

For a given orientation and a given channel (for example BHE) we calculated power spectral densities for every possible combination of day time interval (0h-6h, 6h-12h, 12h-18h, 18h-24h) and season (January-March, April-June, July-September, October-December). This results in 16 different power spectral density distributions for each channel and each orientation that allow us to analyse the seismic noise, for example in summer between 6 in the morning and noon for channel BH and vertical orientation.

The information contained in a single one of these 144 spectra is rather limited. It is more interesting to examine how these spectra vary with time. For the study of seasonal variations it is convenient to compare spectra corresponding to fixed day time intervals, fixed channels, fixed orientations but varying seasons. A scheme of this strategy is shown in table 4.1.

| | January-March | April-June | July-September | October-December |
|---|---|---|---|---|
| 0h – 6h | seasonal variations in the interval from 0:00h to 6:00h | | | |
| 6h – 12h | | | | |
| 12h – 18h | seasonal variations in the interval from 12:00h to 18:00h | | | |
| 18h – 24h | | | | |

**Table 4.1** - *Scheme illustrating the strategy used for the analysis of seasonal variations for a given channel and a given orientation.*

Climate variations at the scale of months with resulting changes in human and industrial activities dominate seasonal variations. For example, the microseismic peaks are usually less pronounced during the summer due to a minor wave activity.

Figure 4.5 illustrates the seasonal variations for the vertical component and the day time interval from 18h-24h. In order to keep this report clear a complete collection of figures showing seasonal variations can be found in *Appendix B*.

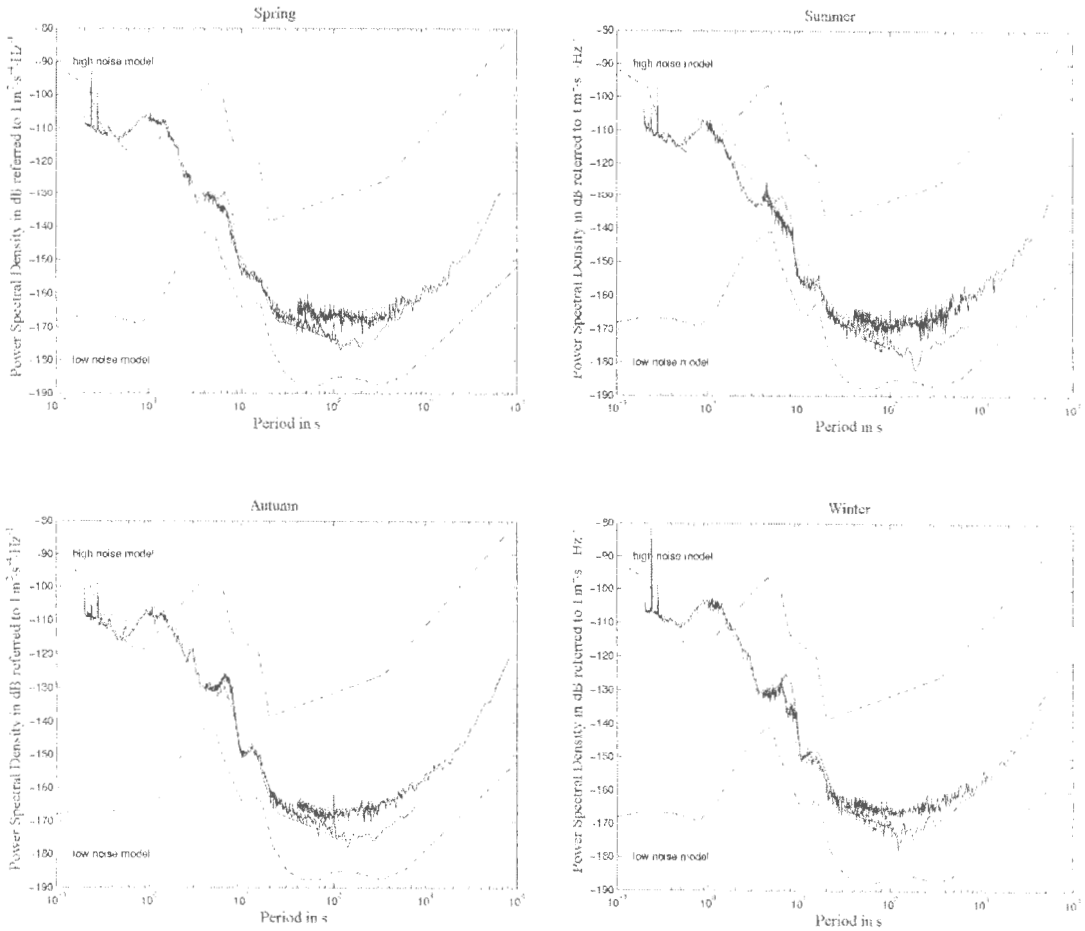


**Figure 4.5** - *Seasonal variations of the vertical component of channels BH and LH for the time interval from 18h-24h. Dashed lines represent* PETERSON'S *(1993) noise models. Dotted lines represent the whole year average for the vertical component.*

The principal characteristics of seasonal variations of seismic noise at station MELI are the following:

1. Throughout almost the whole frequency band the PSD is lower during the summer months and higher during the winter months. This difference can most easily be observed at high frequencies and near the microseismic peaks where seasonal variations amount to as much as 10 dB (figure 4.6). A minor storm and wave activity in the Mediterranean Sea during the summer months seems to be the most likely explanation for these differences near 7 s and 14 s. At low frequencies seasonal variations are less evident, implying that noise sources with periods larger than 1000 s are stable at time scales of various months.

2. Seasonal variations near the microseismic peaks are most evident for the vertical component, suggesting the noise at these frequencies is mainly due to RAYLEIGH waves and not to LOVE waves.

3. The 0.24 s peak shows a strong seasonal variation, implying that it is indeed physical reality and not a numerical error. As we will show later, this peak is almost unrecognizable during the day time interval 0-6 h (figure 4.7) but it is present during

all three remaining day time intervals (6-12 h, 12-18 h and 18-24 h). Moreover, the seasonal variation does not seem to depend significantly on the spatial component, suggesting that the excitation of vertical and horizontal wave field components is similar and temporally stable with respect to the day time interval (at least over the observed time interval).

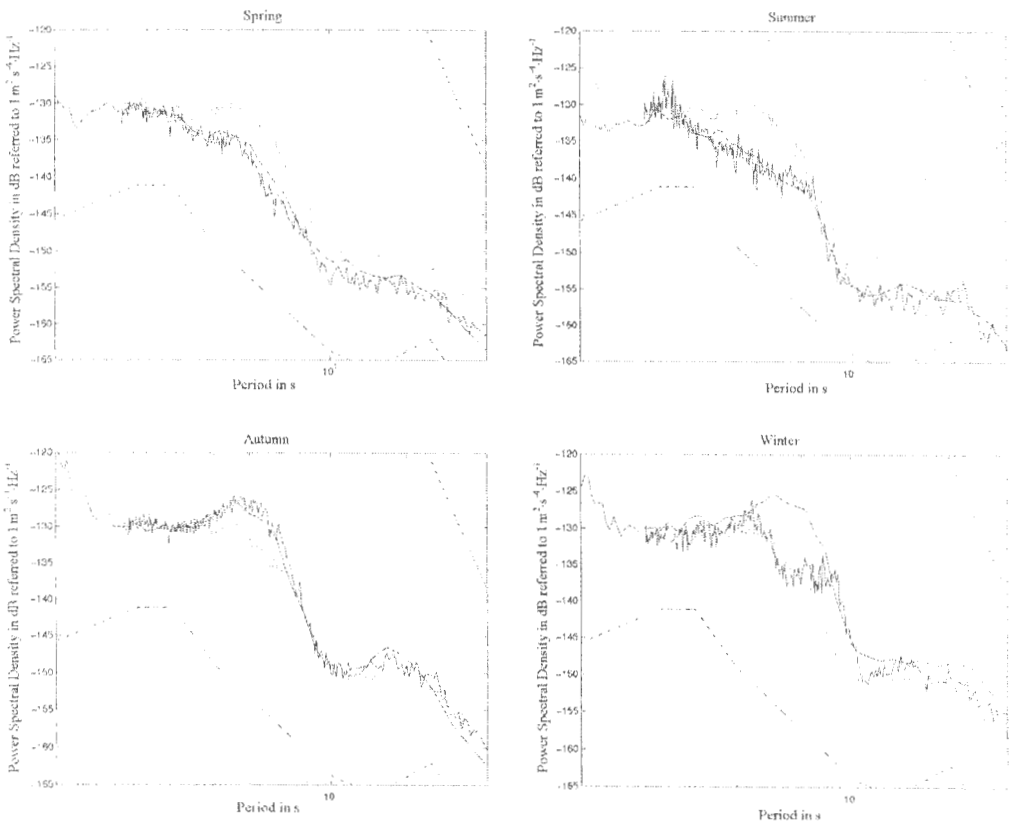


**Figure 4.6** – *Seasonal variations of the vertical component of the channel BH near the microseismic peaks. The chosen time interval is 18h-24h. Dashed lines represent PETERSON'S (1993) noise models. Dotted lineas are the whole year average in PSD for the vertical component.*

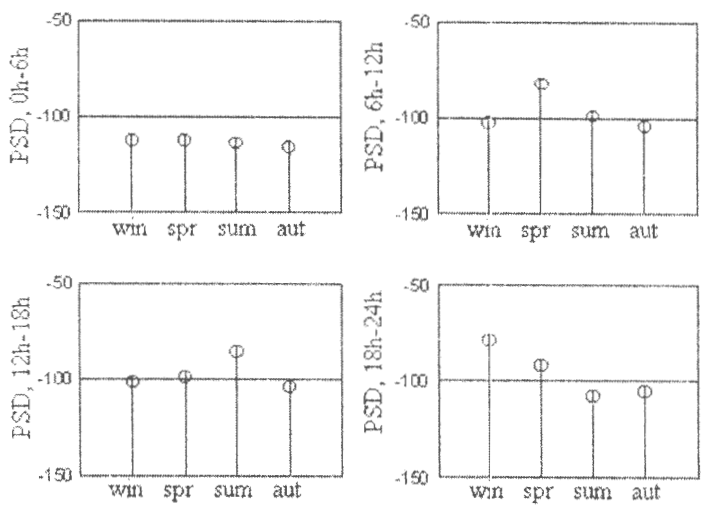


**Figure 4.7** - *Power spectral densities in dB referred to $m^{-2} \cdot s^{-4} \cdot Hz^{-1}$ of the 0.24 s peak for BHE component during different day time intervals. The peak does not exist between midnight and 6 o'clock in the morning.*

As can be seen from figure 4.7 the seasonal variations do not appear to be very systematic. Since we used a robust method to calculate power spectral densities, the seasonal variations of amplitudes of isolated spectral peaks can hardly be interpreted in terms of real physical processes. However, a consistently lower amplitude of the 0.24 s peak during the time interval 0h-6h suggests that human activity is at its origin.

Based on the fact that the noise corresponding to these exceptional peaks is almost monochromatic it is highly probable that the source is of industrial character. Maybe, the nearby electrical power plant operates turbines generating frequency of approximately 4.2 Hz. Between midnight and 6 o'clock in the morning the electric energy consumption might be so low that it is not necessary to use these turbines because another one, corresponding to the 0.28 s peak, guarantees the basic energy production. It is important to note that this, and almost any other interpretation, is nothing more than one of many options. However, it seems relatively plausible.

4. Almost no seasonal variation can be observed at the 0.28 s peak (figure 4.8). In accordance with the above interpretation it might explained with one of the power plant's turbines that operates continuously throughout the whole year.

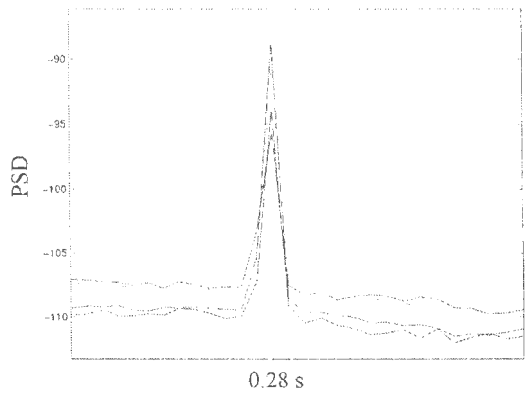


**Figure 4.8** - *Seasonal variations at the 0.28s peak are small compared with variations of the 0.24s peak.*

5. Seasonal variations of the 0.20 s peak are very difficult to verify because it is located right on the edge of the considered frequency band. This in turn makes it necessary to examine whether the 0.20 s peak is physical reality or simply an edge effect.

## 4.3. Daily Variations

Daily variations of seismic noise can be studied in a fashion analogous to the study of seasonal variations. For a given channel, a given orientation and a given season we compare the power spectral densities of seismic noise during the four day time intervals. A scheme of the strategy is shown in table 4.2.

| | January-March | April-June | July-September | October-December |
|---|---|---|---|---|
| 0h – 6h | daily variations in winter | daily variations in spring | daily variations in summer | daily variations in autumn |
| 6h – 12h | | | | |
| 12h – 18h | | | | |
| 18h – 24h | | | | |

**Table 4.2** - *Scheme illustrating the strategy used for the analysis of daily variations for a given channel and a given orientation.*

Since the amount of data for channel LH is insufficient and daily variations for channel VH are meaningless the figures only show power spectral densities for the channel BH. A complete collection of figures showing daily variations can be found in *Appendix C1*.

The principal characteristics of daily variations of seismic noise at station MELI are the following:

1. Daily variations are limited to frequencies above 1 Hz and below 0.1 Hz. In the frequency range 1 Hz > f > 0.1 Hz, daily variations play a minor role and are less systematic. The PSD amplitude is lowest during the early morning hours, i.e. between midnight and 6 am for high and low frequencies (f > 1 Hz and f < 0.1 Hz). An opposite effect can be observed for intermediate frequencies (1 Hz > f > 0.1 Hz). Evidently, three frequency bands have to be considered separately:

   f > 1 Hz : Strong daily variations with magnitudes of 10 dB or more exist for all three orientations and all seasons. These changes in PSD amplitude have classically been attributed to human activity which is lowest during the night and early morning hours and highest during the afternoon. Here, human activity includes traffic and industrial activity.

   1 Hz > f > 0.1 Hz : For intermediate frequencies daily variations are small and not very systematic. The PSD amplitude in this frequency band is almost stable throughout the whole day.

   0.01 < f < 0.1 Hz : Seismic noise at these low frequencies shows various temporal trends. Variations are slightly more pronounced for the horizontal than for the vertical components. Aditionally, a seasonal dependence in daily variations seems to exist. In winter the changes in PSD are smaller than those in spring and summer. For low frequencies, the PSD is smallest between midnight and 6 am. A plausible explanation for these variations are the changing atmospheric conditions, mainly as a consequence of pressure deviations.

2. Easily observable is the dependence of the 0.24 s peak on day time. Between midnight and 6 am this peak is completely absent whereas it can reach a height of more than 20 dB above the normal PSD for the others time intervals.

## 4.4. Daily Variations Based on Modified Intervals

In order to determine if the observed daily variations are indeed caused by human activity one can adapt the conventional subdivision of one day (0-6 h, 6-12 h, 12-18 h, 18-24 h) to the mediterranean way of life. High temperatures during the early afternoon naturally reduce human activity and thus seismic noise. Using the subdivision h1 = 6-14 h, h2 = 14-17 h, h3 = 17-22 h, h4 = 22-6 h, one expects more pronounced temporal variations in the PSDs. Between 22-6 h the seismic noise should be smallest and highest between 6-14 h and 17-22 h. A small reduction of noise can be expected between 14 and 17 h.

However, an analysis of daily variations based on the new intervals did not yield any new results. This implies that the conventional daily intervals are absolutely adequate for the study of daily variations in power spectral density. The results of this calculation for the vertical orientation are summarized in Appendix C2.

## 4.5. Two-factor analysis of seasonal and daily variations

In addition to a qualitative evaluation of temporal variations of seismic noise based on simple observations of power spectral density plots, one can perform a two-factor analysis in order to quantify these results. Since a first evaluation of temporal variations indicated little dependence on spatial orientation and since only few data are available for the LH and VH channels, this two-factor analysis will be applied to the BH recordings only.

A two-factor analysis is based on a simple model of variations of any physical that show changes on at least two different scales. In our particular case the observables are power spectral densities that vary on a daily and seasonal scale. The introduction of such a model has a large number of advantages. It allows to determine to what extent seasonal and daily variations are independent. If these variations are independent to some degree, it allows their separation and quatification. Consequently, it makes possible a more detailed study of temporal effects. This idea is applicable to noise data at other stations, thus paving the way to studies that include quantitative comparisons between stations.

The power spectral density "$X_{ij}(\nu)$" (in dB) in day time interval "i" and season "j" (i,j=1,2,3,4) depends on frequency "$\nu$" and will be expressed in this model as

$$X_{ij}(\nu) = A(\nu) \cdot B_j(\nu) \cdot C_i(\nu) \cdot E_{ij}(\nu).$$

- $A(\nu)$ - average power spectral density for the complete year in dB.
- $B_j(\nu)$ - seasonal variation factor for season "j", does not depend on day time interval "i".
- $C_i(\nu)$ - daily variation factor for the day time interval "i", does not depend on season "j".
- $E_{ij}(\nu)$ - residuals (equal to one if daily and seasonal variations are fully decoupled).

Note that a repeated index does not imply a summation. The "i" index refers to daily interval while "j" refers to seasons. Both range from one to four.

This model needs some explanation in order to understand its significance. In the ideal case, all 16 residuals are equal to one and all temporal variations can clearly be

separated into seasonal variations and daily variations. For example, in the ideal case, the expected PSD for the season "j" for the 6h-12h daily interval can be expressed as $X_{2j}=AB_2C_j$.

At this point we have to deal with a system of 16 equations (one for each $X_{ij}$) and 16 unknowns ($C_i$ and $B_j$) given that all residuals are one. Since these equations represent products and not sums (i.e. they are not linear), there is no unique solution, as one might easily verify.

Thus, it is necessary to find a method that can be used in order to determine a reasonable solution. First, the seasonal variation factor "$B_j$" will be estimated as

$$B_j(\nu) = N_j(\nu)/A(\nu).$$

Where "$N_j(\nu)$" is the average power spectral density of the seismic noise for the season "j". It is obtained by summing the four power spectral densities for this season (one for each daily interval) and then dividing by four. Hence, the seasonal variation factor provides information about how much a seasonal average deviates from the total year average.

$$N_j(\upsilon) = \frac{\sum_{i=1}^{4} X_{ij}}{4}$$

It should noted that "$N_j(\nu)$", as well as "$A(\nu)$", are expressed in dB. The seasonal variation factors "$B_j$" are estimated as a function of "$\nu$". Now, the system contains the same 16 equations but only four unknown factors "$C_i$" that correspond to the daily variations. Evidently, the system is now overdetermined. This implies that a unique solution for "$C_i$", (i=1,2,3,4) can, in general, not be found. As a consequence, residuals "$E_{ij}$" have to be introduced in order to completely describe all daily and seasonal variations. As already mentioned, all 16 residuals are equal to one if seasonal and daily variations are uncorrelated. An approxiamte solution for the daily variation factors can be found in a least squares sense. Since the ideal case is $E_{ij}=1$ for all i,j=1,2,3,4, it is reasonable to find an approximate solution such that the sum of absolute differences between 1 and $E_{ij}$ is minimized, i.e.

$$R(E_{ij}) := \|1\text{-}E_{ij}\|_2 = [(1\text{-}E_{11})^2 + (1\text{-}E_{12})^2 + \ldots + (1\text{-}E_{44})^2]^{1/2} = \min!.$$

Using the relations $R(E_{ij}) = R(X_{ij} \cdot A^{-1} \cdot B_j^{-1} \cdot C_i^{-1})$ and $dR(E_{ij})/dC_i = 0$ for all i=1,2,3,4, one can easily find the solution of this least squares problem:

$$C_i = \frac{\sum_{j=1}^{4} (X_{ij} \cdot A^{-1} \cdot B_j^{-1})^2}{\sum_{j=1}^{4} X_{ij} \cdot A^{-1} \cdot B_j^{-1}}$$

First, let us analyse the seasonal averages $N_j(\nu)$. The results for the four intervals January-March, April-June, July-September and October-December can be seen in figure 4.9.

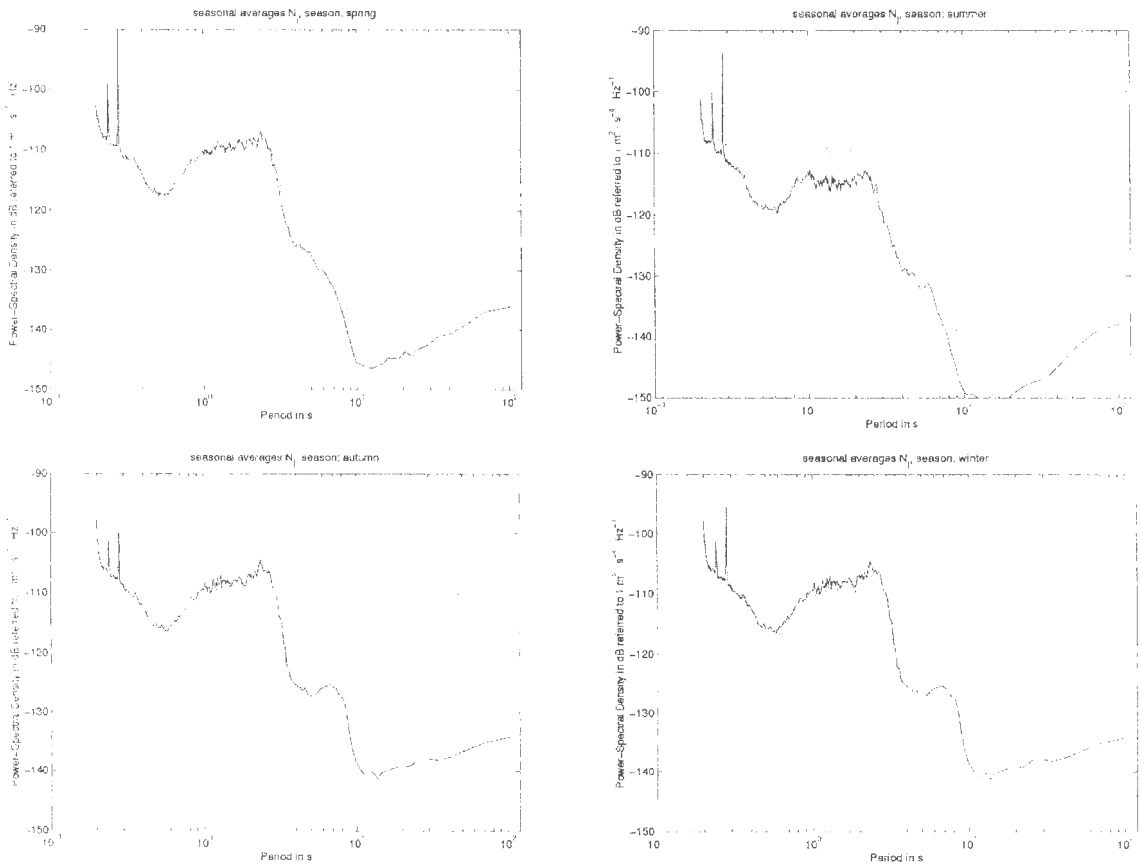


**Figure 4.9** - *Seasonal averages of the channel BHE. Dotted lines represent the whole year average for the same channel. Seasons from top left to bottom right: spring, summer, autumn, winter.*

As we observed previously, the PSD is highest during winter throughout almost the complete spectrum. For periods smaller than 1 s seasonal differences are practically negligible, the only exception being summer. This may be due to a smaller human and industrial activity during the warm season. However, for periods between 1 s and 3 s, the noise power spectral density during the summer is significanly lower than during all the other seasons. Evidently, a certain source of seismic noise that generates those frequencies is not present in summer. Another interesting feature is the 7 s peak which is relatively pronounced in autumn and winter and as good as absent in spring and summer. This effect can probably be attributed to a more moderate weather and less intense ocean wave activity between April and September. It is relatively difficult to uniquely interpret the strong seasonal variations at periods from 10 s to 100 s. The list of possible noise sources goes from human activity over electric power plants to climate related effects.

The plots showing the seasonal correction factors (figure 4.10) emphasize the results already mentioned above and moreover, it adds new quantitative information.

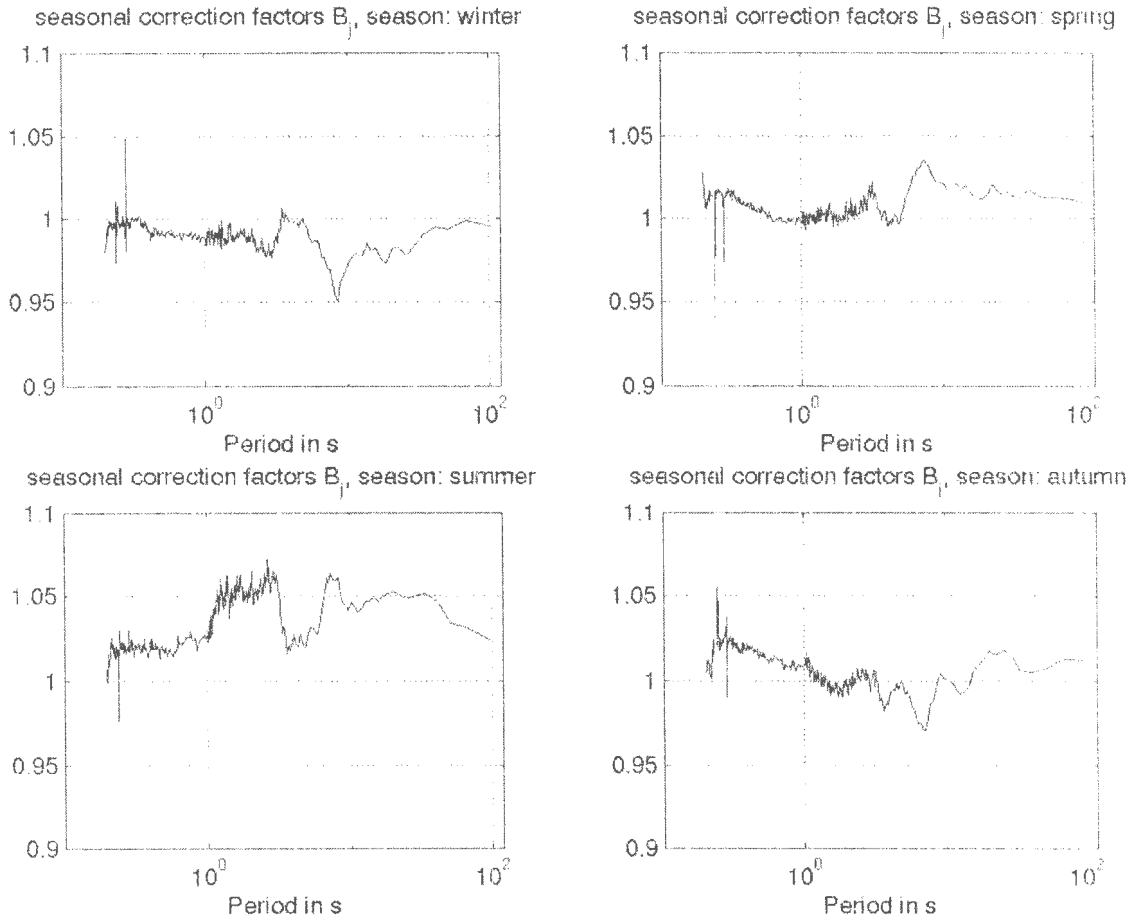


**Figure 4.10** - *Seasonal correction factors for the channel BHE. Values of B larger than 1 imply a lower PSD because the scale is in dB.*

For periods between 1 and 3 seconds, the power spectral density of the noise during the summer of 2000 can be estimated to be approximately 6% lower than in winter, spring and autumn. (Note that large B values imply a smaller PSD. This is true because it is measured in dB and atteins negative values throughout the considered frequency band. Hence, multiplication by a number larger than one yields even more negative, i.e. smaller values.) The difference in PSD between summer and winter for periods larger than 10 s is as big as 8%. The amplitude of the 7 s peak varies up to 10% over one year with respect to the one year average.

Very interesting is the seasonal variation of the 0.24 s peak, where "$B_j$" reaches values of more than 1.05 in autumn and 0.94 in spring. A completely different behaviour can be observed for the peak at roughly 0.28 s, as can be seen in figure 4.11. As mentioned before, we think that these exceptional peaks are caused by the electric power plant near the seismic station. It might be a turbine which could generate the nearly monochromatic noise represented by these peaks.

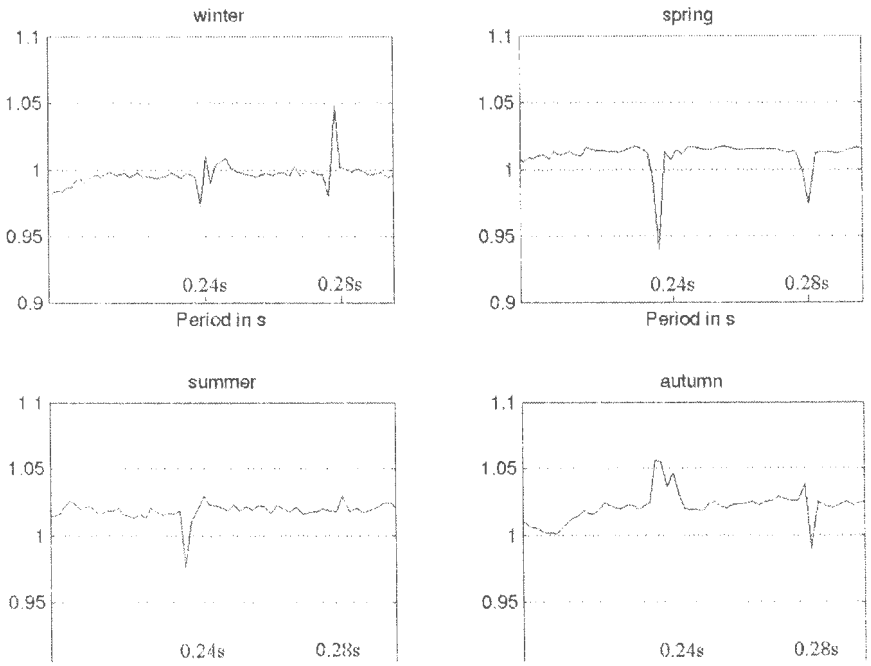


**Figure 4.11** - *Seasonal correction factors. Magnification of 0.24 s and 0.28 s peaks.*

The next step is to analyse the daily variation factors $C_i(\nu)$ and the residuals $E_{ij}$ (figure 4.12).

The highest $C_i$ values are reached during the night interval (0h- 6h) for the low and high frequency bands, while in the intermediate band (0.6 – 8 s) the daily variation factor is less than one. This means that the expected PSD is higher in the intermediate band and lower in the low and high frequency bands.

In the 6h - 12h interval the situation changes completely, the daily variation factor being less than one in the low and the high frequency bands and larger than one in the intermediate band.

For the 12h -18h interval the factor is always less than one, being very close to one in the intermediate band. In the 18h - 24h interval the factor remains larger than one for the whole considered frequency band.

The daily variation factors behave as one would expect in the low and high frequency bands, being larger than one during the night when the human activities decay and less than one during the working hours.

Also from 12h to 24h the factors behave as one may expect, being less than one during working time and higher at night. In both intervals, this factor is very close to one, meaning that the daily human activity does not have a large influence in the studied range of frequencies.

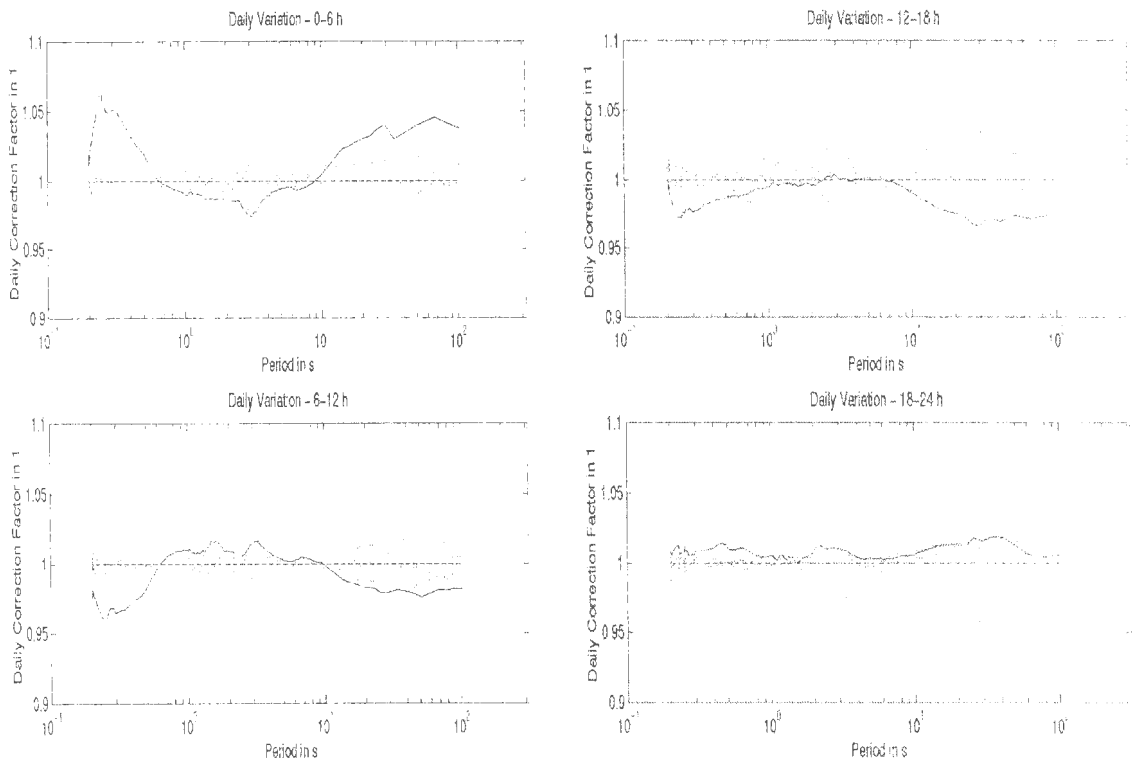


**Figure 4.12** - *Daily variation factors (solid lines). Dotted lines represent the four residuals corresponding to each of the factors. All curves have been smoothed: Each point is the arithmetic mean of itself and the 14 neighboring points.*

For periods between 1s and 10s an explanation of the observed variations in the 0h-6h and 6h-12h intervals is more difficult and less certain. From 0h to 6h, the factor remains less than one (meaning that the PSD is higher than the average) while it is higher than one from 6h to 12 h. We think that these unexpected values could be due to temperature changes, in spite of the fact that the sensor is isolated with a polystyrol box and an aluminium helmet with rubber foam inside (Hanka, 2002).

The residuals are not close to 1 for most of the frequency band. However, it is interesting to take a closer look: Since the residuals are factors and not summands, as they usually are, we lack intuition of what their amplitudes mean in terms of model fit.

In figure 4.13 we compare the PSD of channel BHE in summer between 6h and 12h to the respective model without residuals, i.e.

$$M_{ij}(\nu) = A(\nu) \cdot B_j(\nu) \cdot C_i(\nu), \qquad i = 2, \quad j = 3.$$

First, we note that the model-data fit is acceptable even in period ranges where the residuals are larger, namely between 1s and 10s. Indeed, the differences in most of the considered period band are recognizable only in a magnification, which is shown on the right hand side. This implies that the model is indeed adequate, the exceptions being periods larger than 10s and a narrow band around 1s.

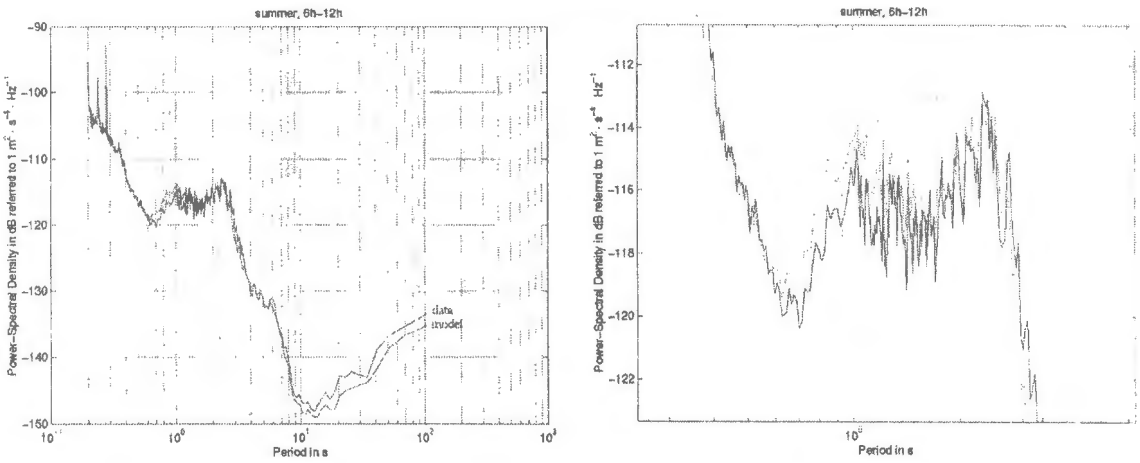


**Figure 4.13** - *Comparison between the PSD for channel BHE in summer for the interval 6h-12h ($X_{23}(\nu)$) and the model without residuals ($M_{23}(\nu)$). The figure on the left shows a magnification for periods around 1s. The solid curve represents the data and the dotted curve represents the model without residuals.*

## 5. Delta function experiment

The observation of unusually high peaks in the noise power spectral density and the discrepancies between the estimated PSD for the LH and VH channels suggest that the numeric estimation of the noise power spectral densities might introduce some errors. In order to check the exactness of these calculations, we have calculated the PSD using a delta impulse (synthetic noise) as the input. Since the delta impulse contains all frequencies equally weighted the resulting power spectral density should be very simple, and it should have the same shape and values for all components, because the frequency response of the sensor at station MELI (figure 5.1) is identical for all components. Moreover, it should be a continuous function for the whole spectral band. The result of this test can be seen below, in figure 5.2.

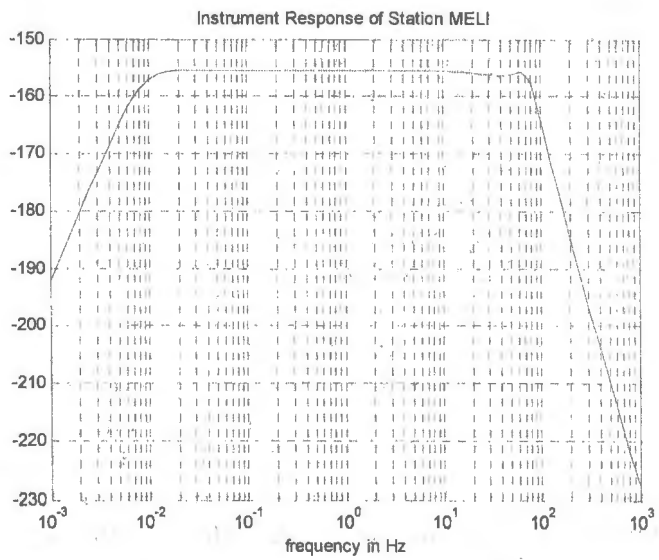


**Figure 5.1** - *STS2 sensor response for station MELI. The response is identical for all components (E/W, N/S, and the vertical, Z).*

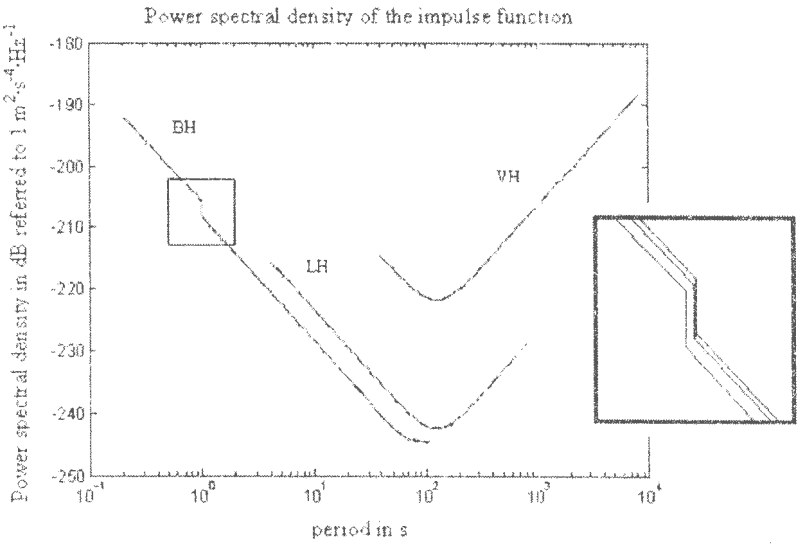


**Figure 5.2** - *Power spectral densities calculated for a discrete impulse of amplitude one. The procedure used is identical to that one applied to the real data. The schematic magnification of the boxed part of the diagram reveals that there are three different curves for each channel, corresponding to the respective orientations.*

A brief look at this result reveals that something went wrong. The directly observable errors are:

i) For each channel (BH, LH, VH) three different curves corresponding to the three different orientations (E, N, Z) appear. The difference between these curves is approximately 1.5 dB to 3.0 dB. Admittedly, these differences are small compared to the amplitude of the actual data. Their origin is unclear.

ii) The curves for channel BH show a discontinuity of –2.8 dB at a period of exactly 1 s.

iii) Instead of a continuous curve composed of three curves (one for each channel) we observe three isolated groups of curves. Each corresponding to one channel (BH, LH or VH) and comprising three slightly different curves, one for each orientation (E, N or Z). Undoubtedly, this is the most significant error.

For comparison, the shape of the theoretical power spectrum can be seen in figure 5.3. One reason for these differences between the theoretical prediction and the numerical realization might be the frequency content of the delta impulse which is undoubtedly unusual for a seismogram. Maybe, the program that calculates the power spectral densities could cannot handle frequencies of 1000 Hz contained in a seismogram that has an expected frequency band of 0.001 Hz to 0.125 Hz (for channel LH). For this reason, we applied a band-pass filter (antialiassing filter) to the delta functions in order to eliminate unrealistic frequencies. The normal frequency content for all three different channels is summarized in table 5.1. Unfortunately, this modification does not result in correct power spectral densities, as can be seen in figure 5.4. All errors mentioned before appear in exactly the same form. Solely, the effect of filtering the delta functions can be observed near the cut-off frequencies of the respective channels.

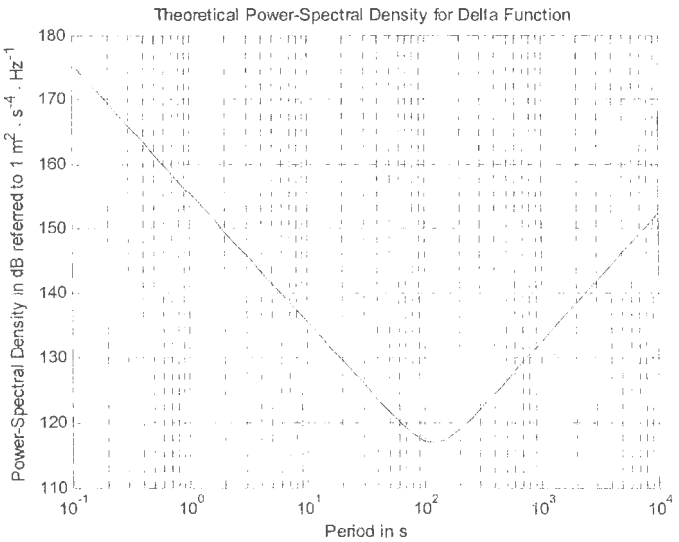


**Figure 5.3** - *Theoretical power spectral density as a function of period for a unit impulse. The absolute values of the PSD depend on a scaling factor that has not been taken into account, resulting in a vertical translation of the curve. However, the shape is correct.*

| Channel | Frequency Band (Hz) |
|---|---|
| **BH** | 0.01 – 4.0 |
| **LH** | 0.001 – 0.125 |
| **VH** | 0.0001 – 0.002 |

**Table 5.1** - *Frequency ranges of the channels BH, LHand VH.*

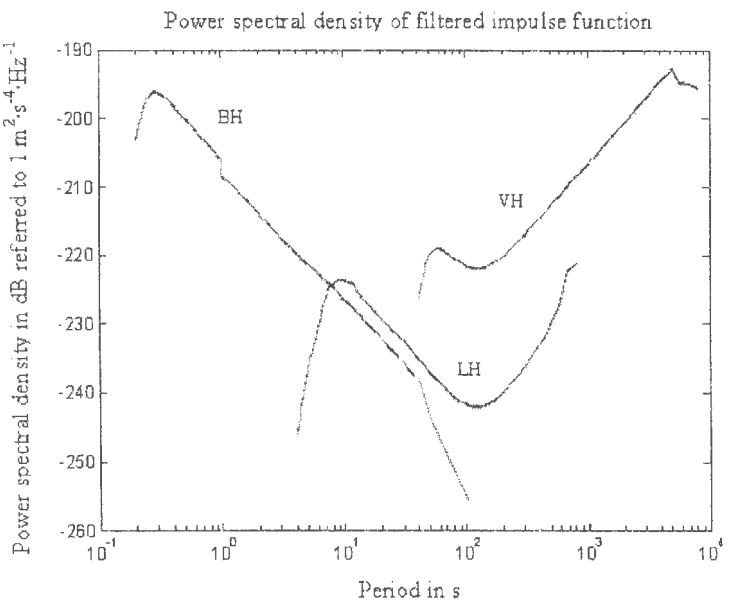


**Figure 5.4** - Power spectral densities estimated for the filtered unit impulses.

The fact that we used only one synthetic seismogram for each component and each channel may contribute to these erroneous results. However, the differences between different channels should not depend on the number of recordings used.

These preliminary results should be treated carefully, requiring a deep revision of the used synthetic noise (delta function) and also of the used programs. Additionally, numerous tests should be carried out in order to guarantee the accuracy of future studies.

## 6. Effects of digital filters

The prominent peaks that can be observed in the power spectral densities of various channels can possibly be explained by taking all the different filters into account that have been applied to the digital signal. In the process of computing the power spectral density only the effect of the instrument response has been removed. However, the effects of other digital filters are still included in the spectrum.

The filters (Figure 6.1 shows an example.) belong to the acquisition system and are constructed such that they are practically plane with unit magnitude for a certain frequency range and than almost zero for all frequencies higher than the cutoff frequency $f_0$ As a result, frequencies higher than $f_0$ should theoretically not be present in the seismograms used to compute the power spectral density. Practically however this is not the case because the filters are not perfect. Moreover, the extensive signal processing adds numeric noise that becomes comparable to the natural noise at frequencies higher than the filter cutoff frequency. Consequently, the power spectral densities are reliable only up to a certain frequency even though the calculation may yield results for higher frequencies.

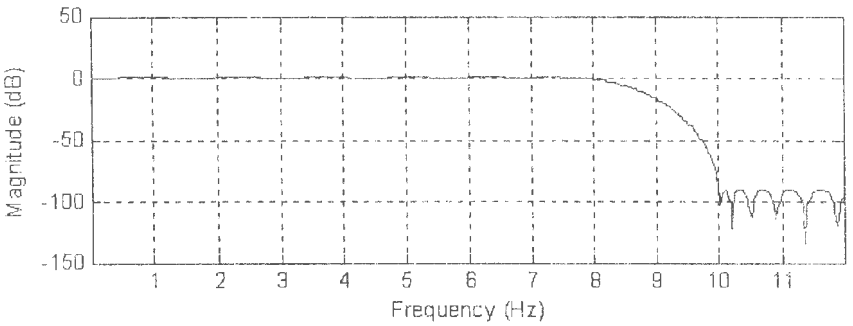


**Figure 6.1** - *Last filter stage for station MELI (channel BH, orientation E). The cut-off frequency is approximately 8 Hz.*

In the case of channels BHE, BHN and BHZ of station MELI this frequency limitation is set by the last filter stage. As can be seen in figure 6.1, all contributions to the signal with a frequency above 8 Hz (period of 0.125 s) are practically eliminated by the FIR filters.

The power spectral densities obtained previously for channel BHE (see for example figure 4.1) reveal that the observed peaks cannot have their origin in the phenomenon described above because the highest frequencies contained in the power spectrum are

below 8 Hz and hence reliable. In particular, the peak at 0.2 s cannot be an edge effect related to digital filters.

## 7. Conclusions

The seismic noise recorded during the year 2000 at the broadband station MELI has been studied on the basis of power spectral density estimations.

Throughout the considered frequency band power spectral densities are high, the only exception being the vertical component of channel VH. Due to anthropogenic noise sources in the vicinity of the station, power spectral densities of all orientations (E, N, Z) even exceed the reference values given by PETERSON (1993) in a period range from 0.2 s to 2.1 s. Various prominent peaks (at periods of 0.20 s, 0.24 s and 0.28 s) also seem to be related to human activity (an electric power plant). The majority of the observed temporal variations can be explained by changes in human activity and atmospheric conditions. However, one should keep in mind that most interpretations offered here are not unique.

Based on a two-factor analysis one finds that anthropogenic noise is prominent only in a very restricted frequency band between 2 Hz and 5 Hz. Daily variations outside this band are characterized by significant seasonal variations.

Power spectral density estimations for unit impulse functions reveal numerical problems. These irregularities in the calculation process may be responsible for some of the characteristics of the power spectral density plots such as the differences between channels LH and VH in the overlapping frequency band.

# Appendix A

# Appendix A – Complete Year

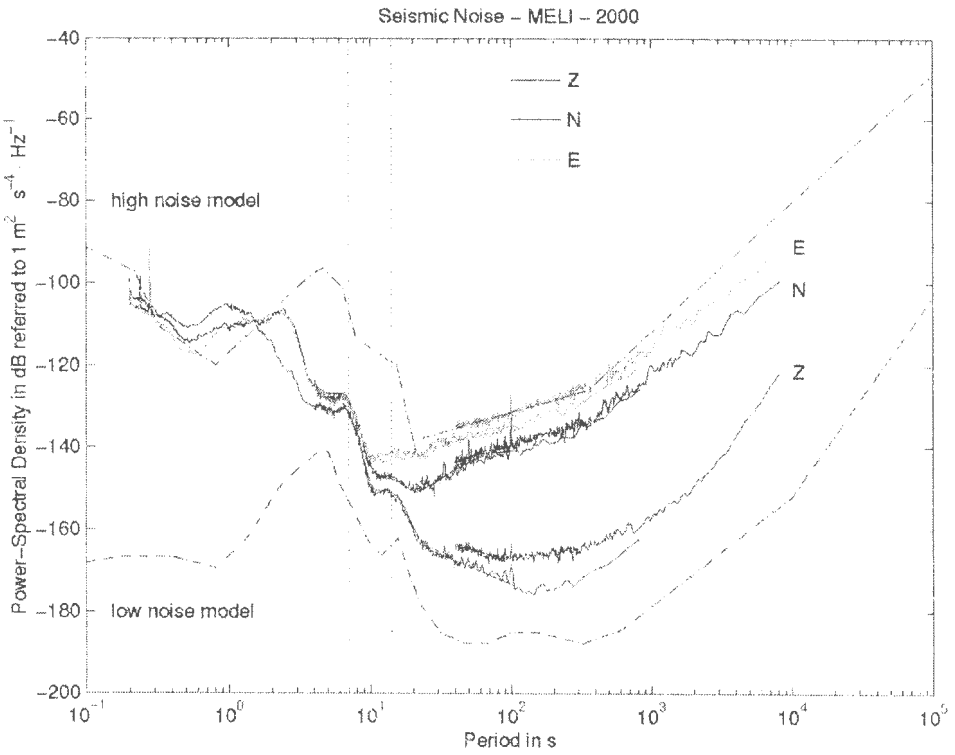


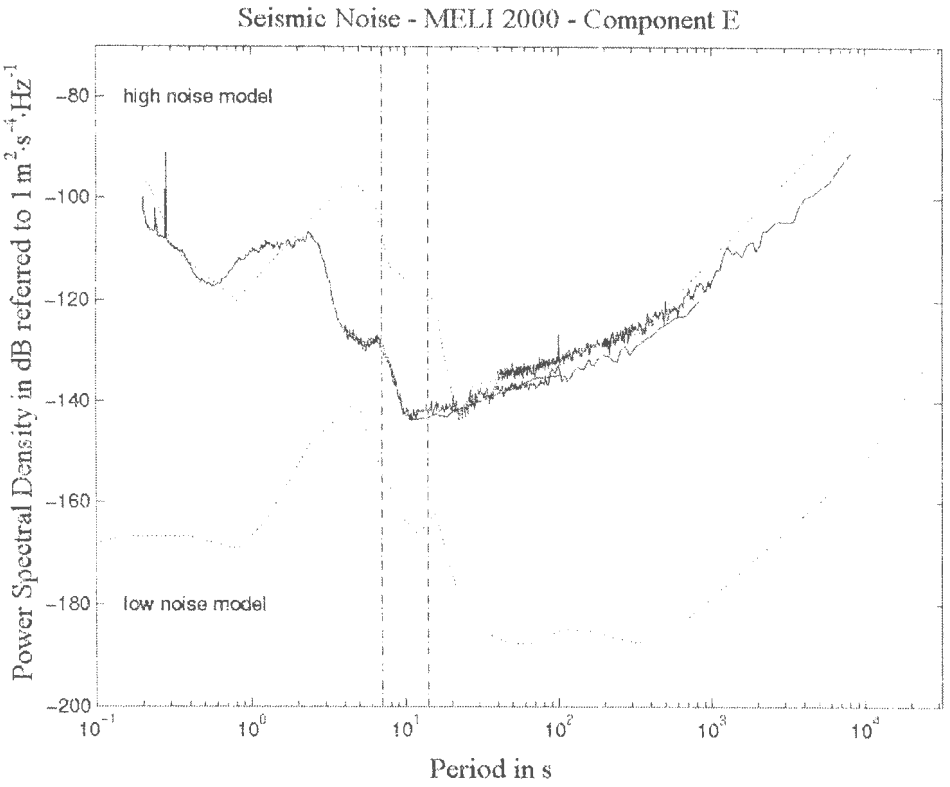

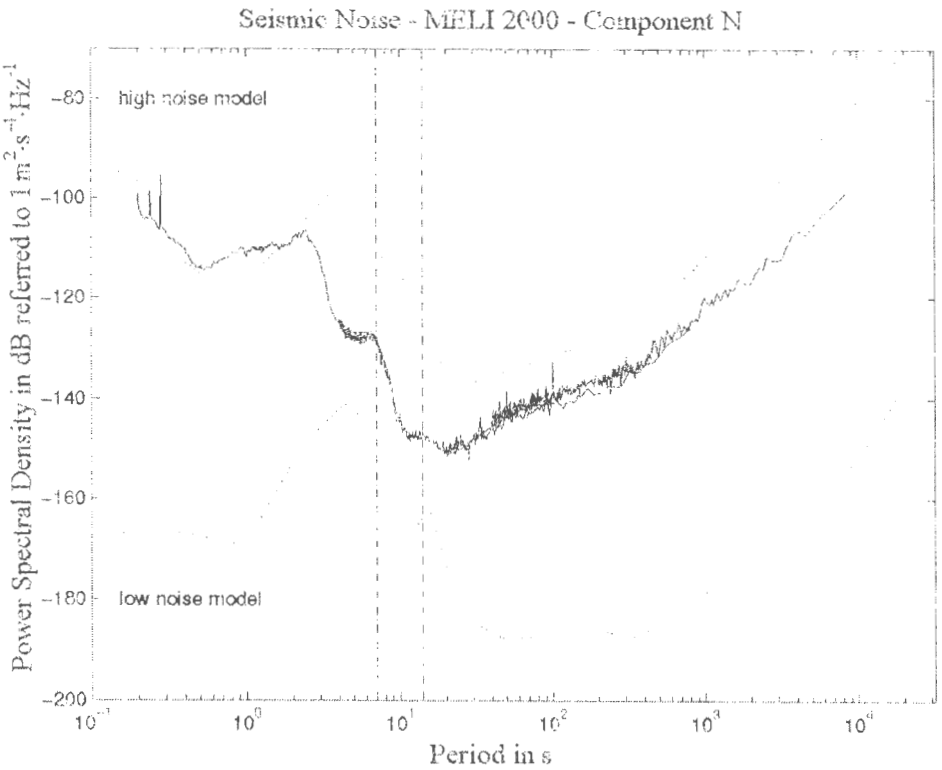
Seismic Noise - MELI 2000 - Component N
high noise model
low noise model
Power Spectral Density in dB referred to 1 m²·s⁻⁴·Hz⁻¹
Period in s
-80
-100
-120
-140
-160
-180
-200
10⁻¹
10⁰
10¹
10²
10³
10⁴

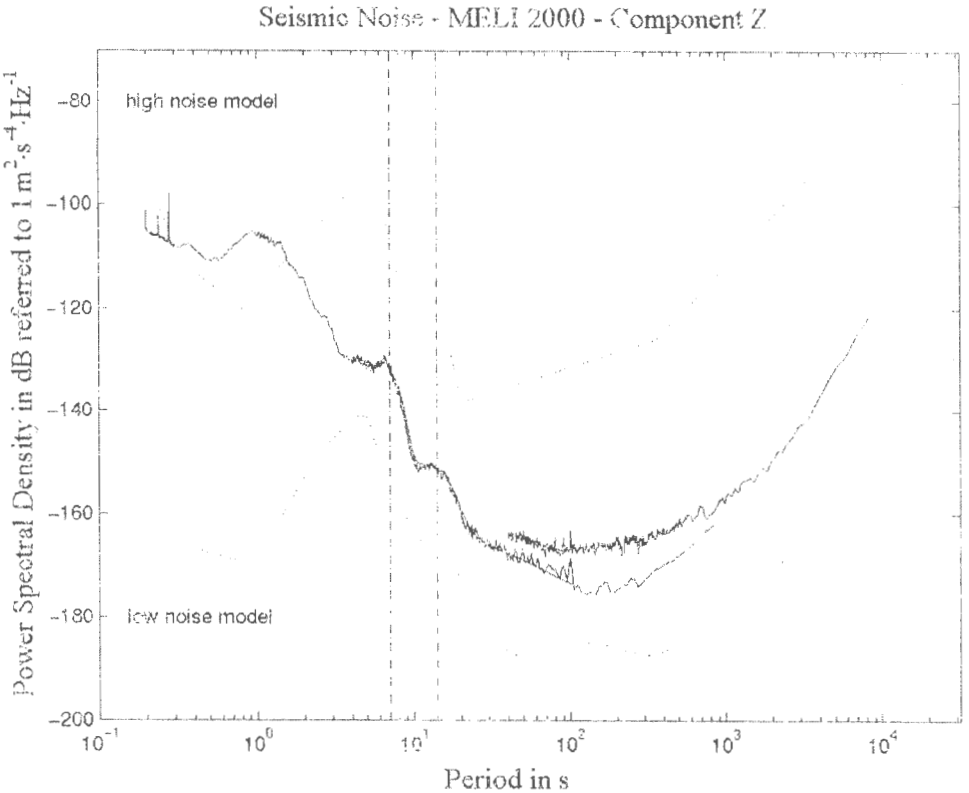
Seismic Noise - MELI 2000 - Component Z
high noise model
low noise model
Power Spectral Density in dB referred to 1 m²·s⁻⁴·Hz⁻¹
Period in s
-80
-100
-120
-140
-160
-180
-200
10⁻¹
10⁰
10¹
10²
10³
10⁴

# Appendix B

# Appendix B – Seasonal variations

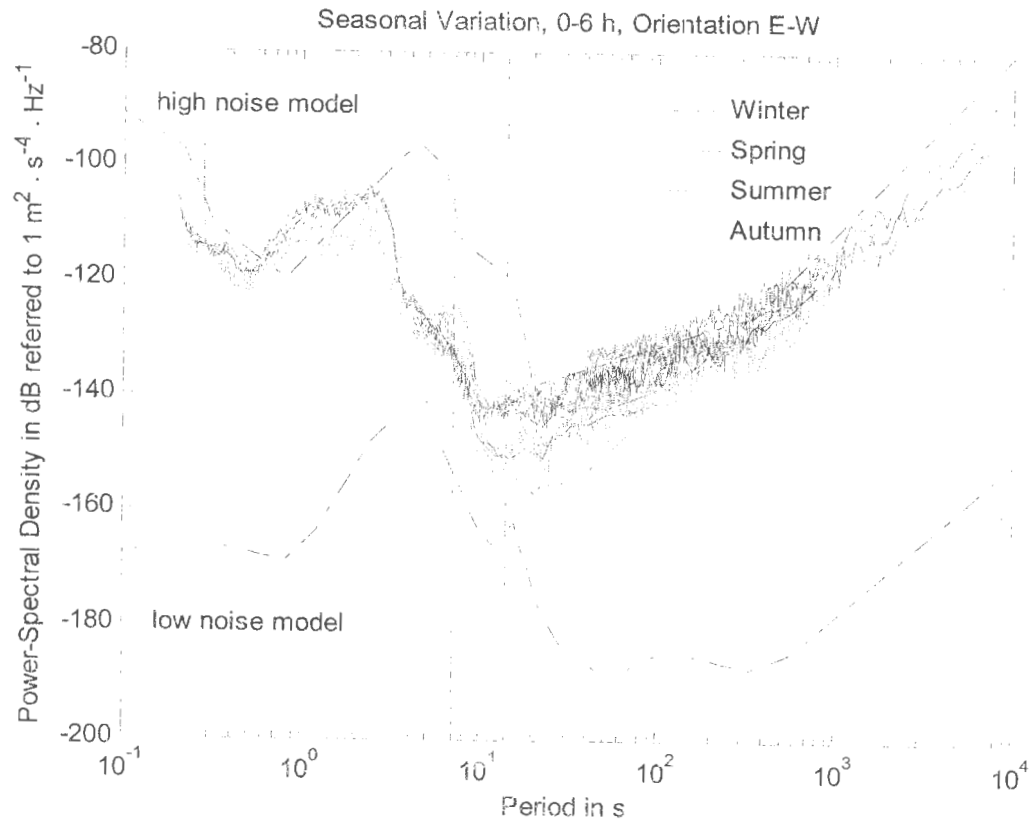


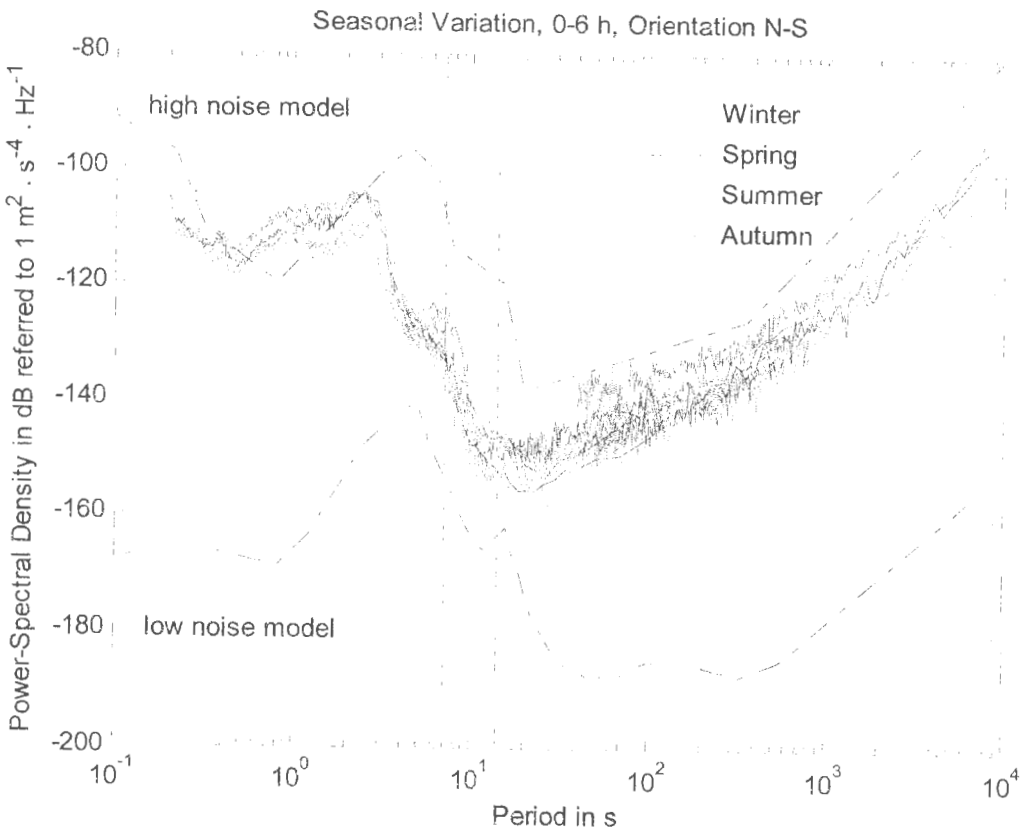

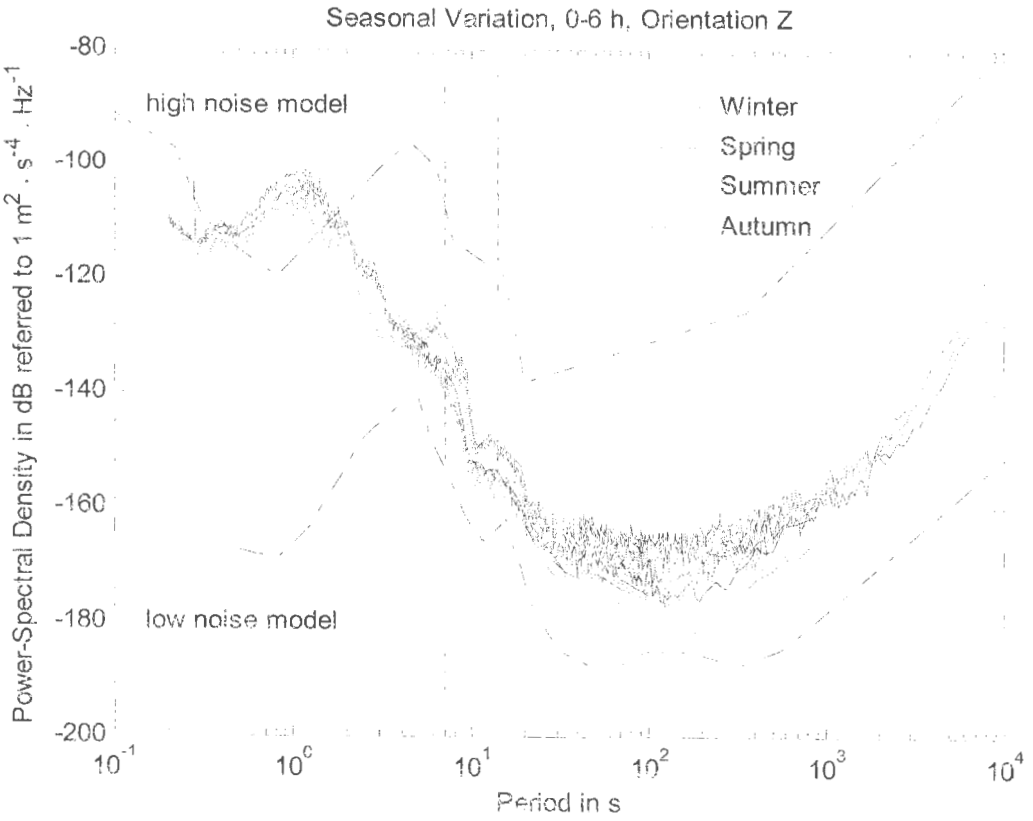
Seasonal Variation, 0-6 h, Orientation Z
high noise model
low noise model
Winter
Spring
Summer
Autumn
Power-Spectral Density in dB referred to 1 m² . s⁻⁴ . Hz⁻¹
Period in s
-80
-100
-120
-140
-160
-180
-200
10⁻¹
10⁰
10¹
10²
10³
10⁴

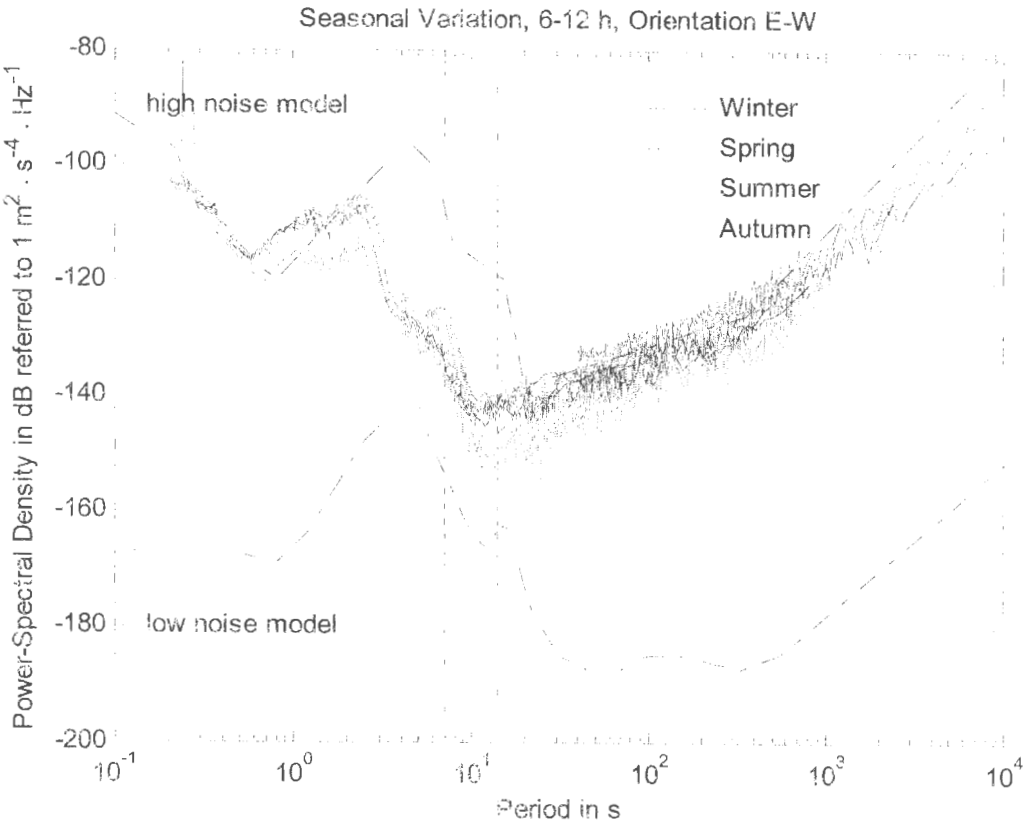
Seasonal Variation, 6-12 h, Orientation E-W
high noise model
low noise model
Winter
Spring
Summer
Autumn
Power-Spectral Density in dB referred to 1 m² . s⁻⁴ . Hz⁻¹
Period in s
-80
-100
-120
-140
-160
-180
-200
10⁻¹
10⁰
10¹
10²
10³
10⁴

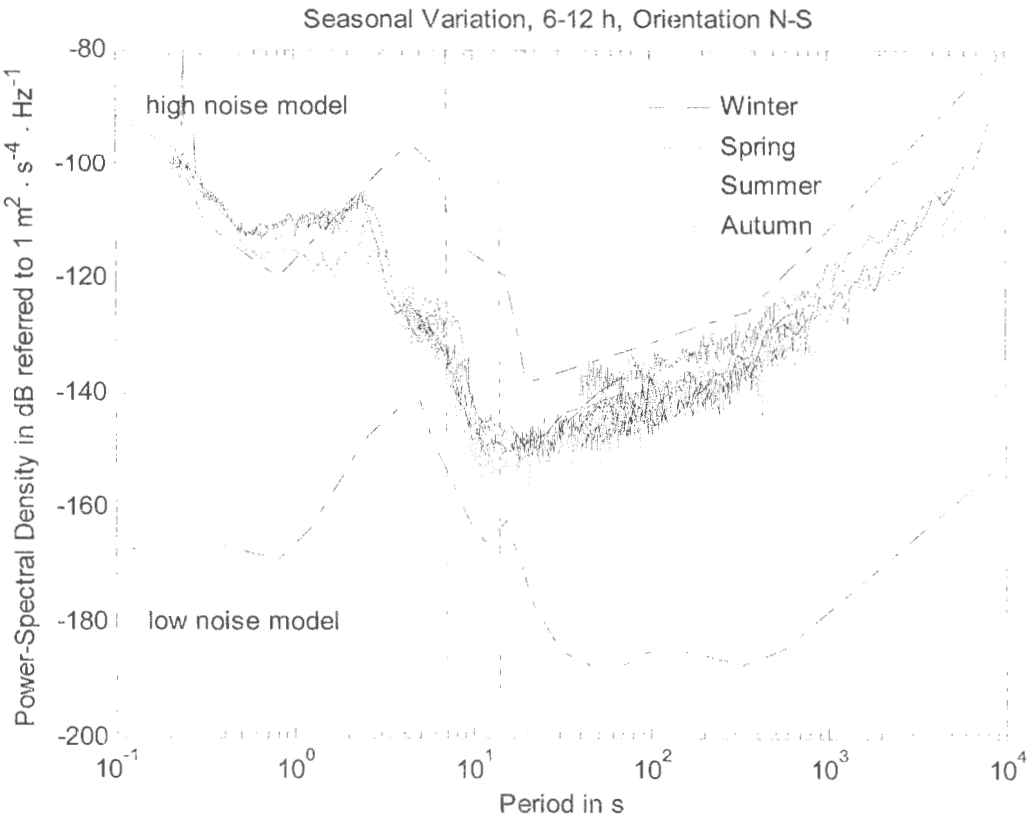
Seasonal Variation, 6-12 h, Orientation N-S
high noise model
low noise model
Winter
Spring
Summer
Autumn
Power-Spectral Density in dB referred to 1 m² . s⁻⁴ . Hz⁻¹
Period in s
-80
-100
-120
-140
-160
-180
-200
10⁻¹
10⁰
10¹
10²
10³
10⁴

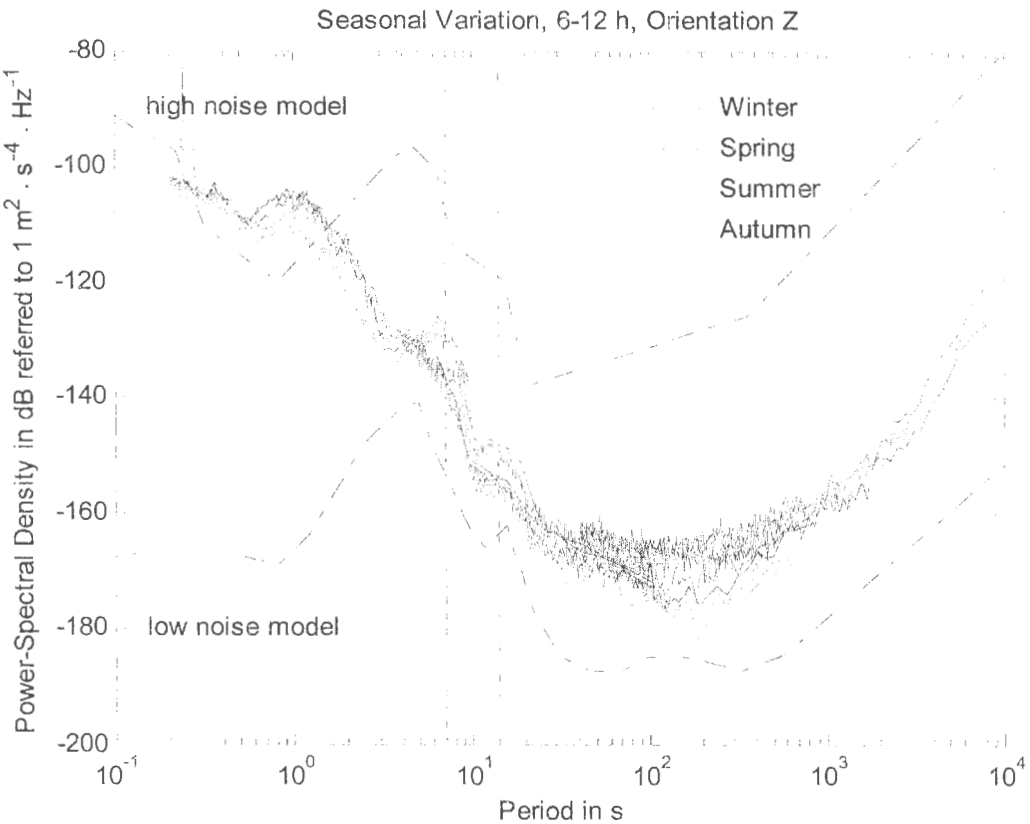
Seasonal Variation, 6-12 h, Orientation Z
high noise model
low noise model
Winter
Spring
Summer
Autumn
Power-Spectral Density in dB referred to 1 m² . s⁻⁴ . Hz⁻¹
Period in s
-80
-100
-120
-140
-160
-180
-200
10⁻¹
10⁰
10¹
10²
10³
10⁴

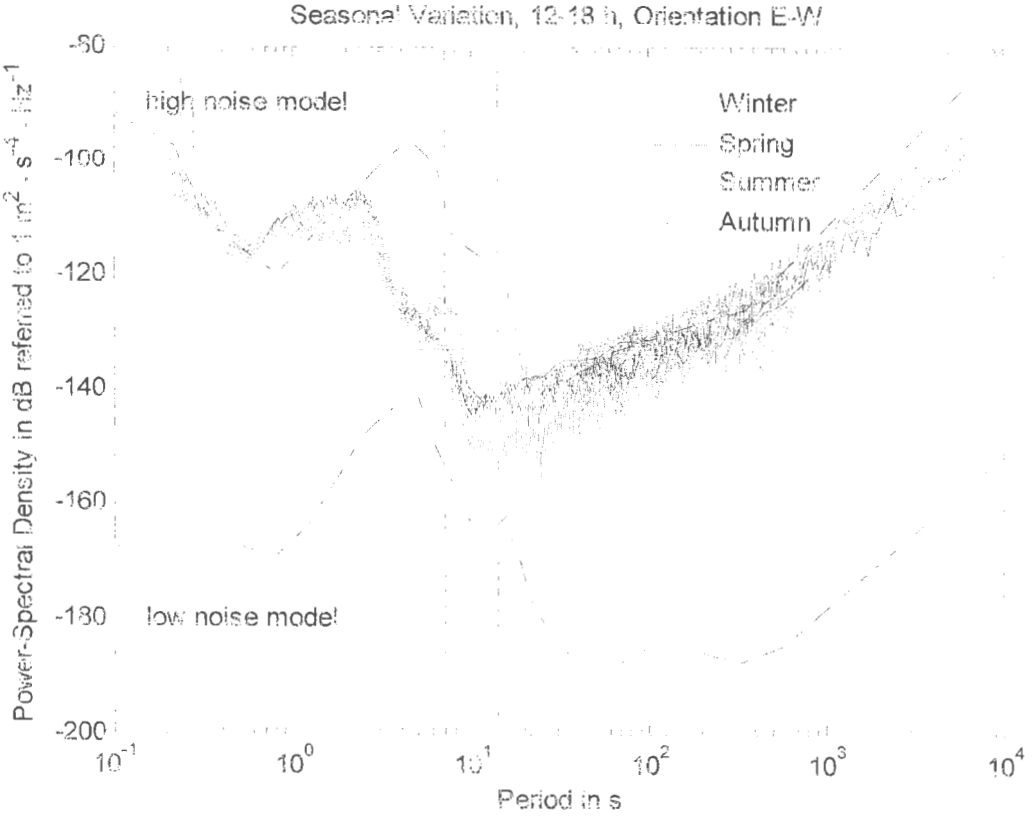
Seasonal Variation, 12-18 h, Orientation E-W
high noise model
low noise model
Winter
Spring
Summer
Autumn
Power-Spectral Density in dB referred to 1 m² · s⁻⁴ · Hz⁻¹
Period in s
-80
-100
-120
-140
-160
-180
-200
10⁻¹
10⁰
10¹
10²
10³
10⁴

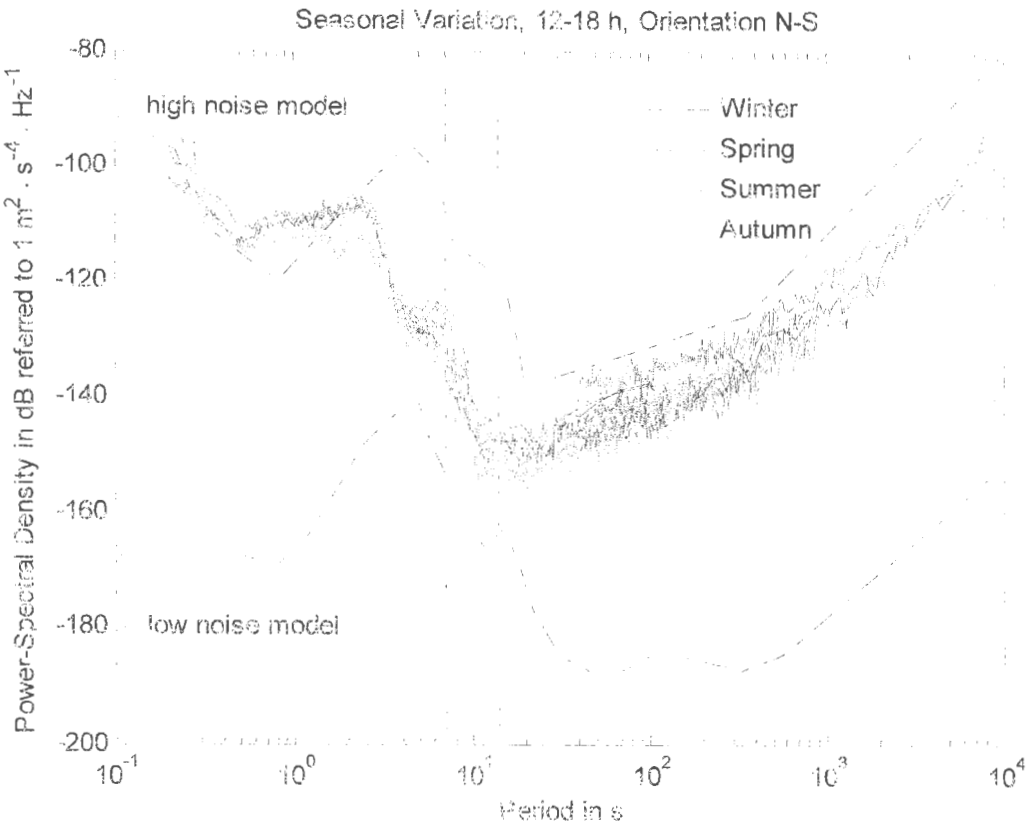
Seasonal Variation, 12-18 h, Orientation N-S
high noise model
low noise model
Winter
Spring
Summer
Autumn
Power-Spectral Density in dB referred to 1 m² · s⁻⁴ · Hz⁻¹
Period in s
-80
-100
-120
-140
-160
-180
-200
10⁻¹
10⁰
10¹
10²
10³
10⁴

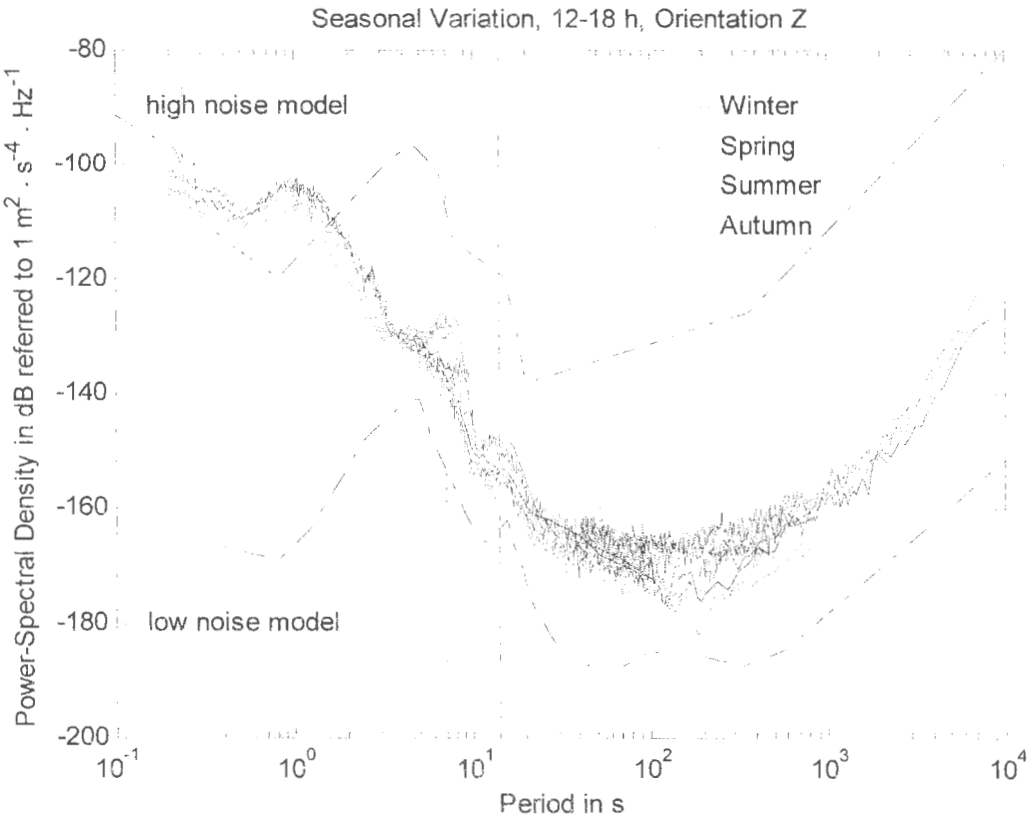
Seasonal Variation, 12-18 h, Orientation Z
high noise model
low noise model
Winter
Spring
Summer
Autumn
Power-Spectral Density in dB referred to 1 m$^2$ . s$^{-4}$ . Hz$^{-1}$
Period in s

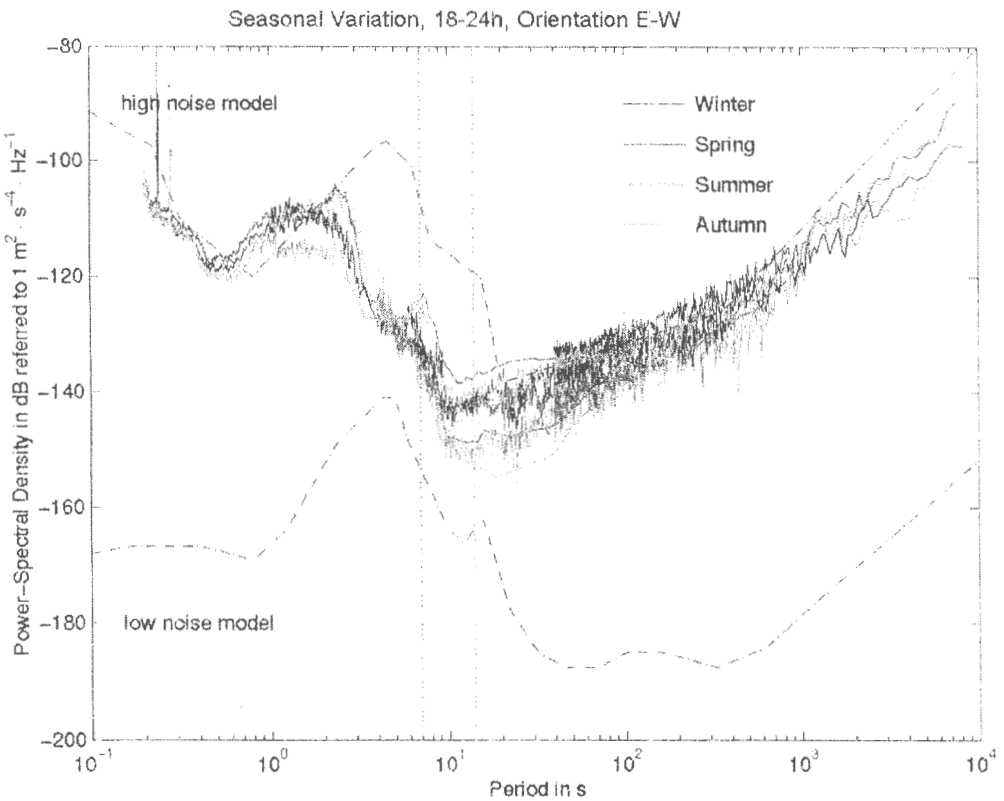
Seasonal Variation, 18-24h, Orientation E-W
high noise model
low noise model
Winter
Spring
Summer
Autumn
Power-Spectral Density in dB referred to 1 m$^2$ . s$^{-4}$ . Hz$^{-1}$
Period in s

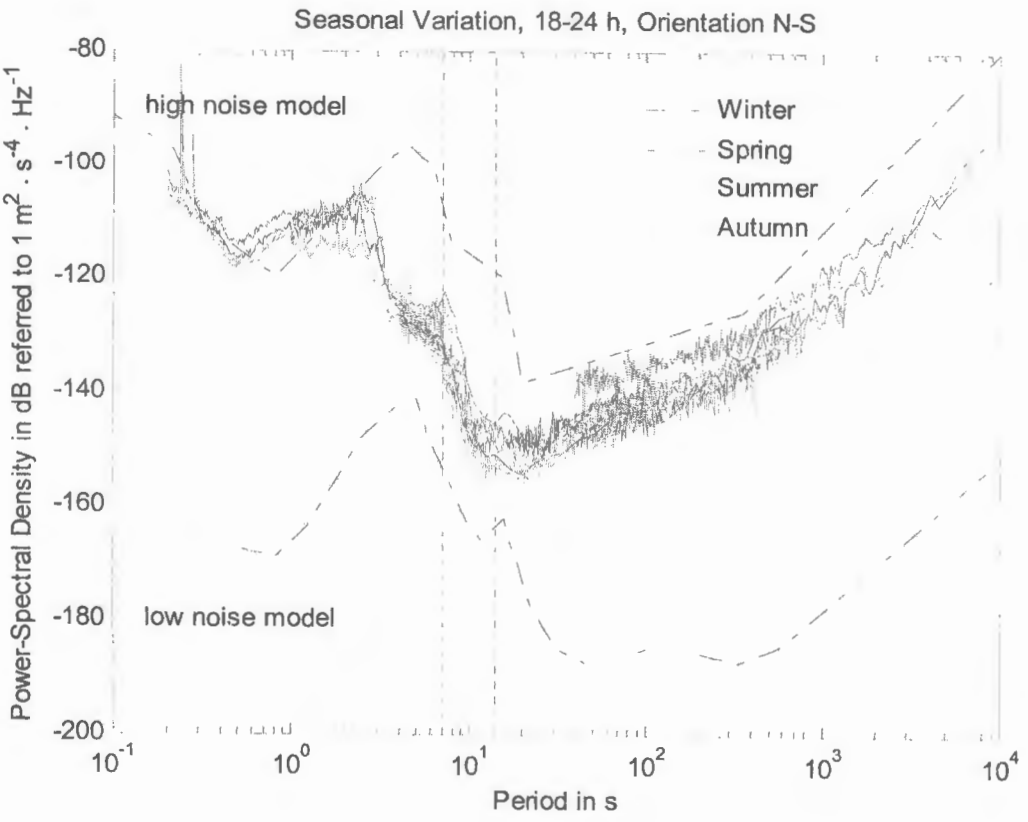
Seasonal Variation, 18-24 h, Orientation N-S
high noise model
low noise model
Winter
Spring
Summer
Autumn
Power-Spectral Density in dB referred to 1 m² . s⁻⁴ . Hz⁻¹
Period in s

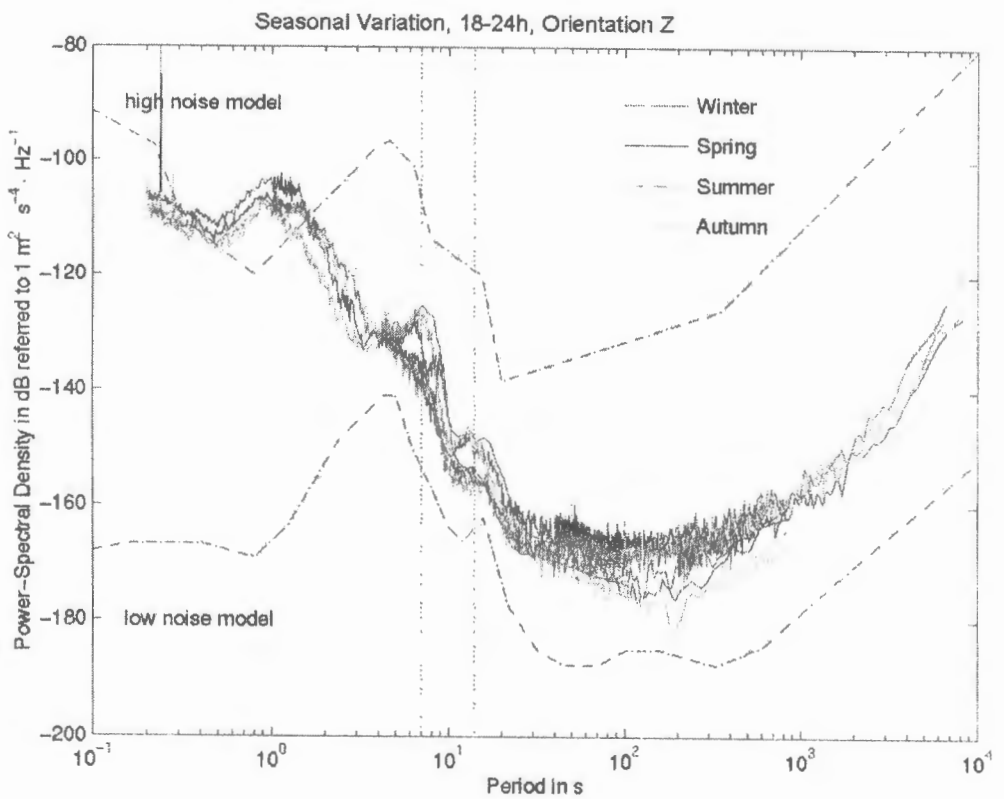
Seasonal Variation, 18-24h, Orientation Z
high noise model
low noise model
Winter
Spring
Summer
Autumn
Power-Spectral Density in dB referred to 1 m² s⁻⁴ . Hz⁻¹
Period in s

# Appendix C1

# Appendix C1 – Daily variations

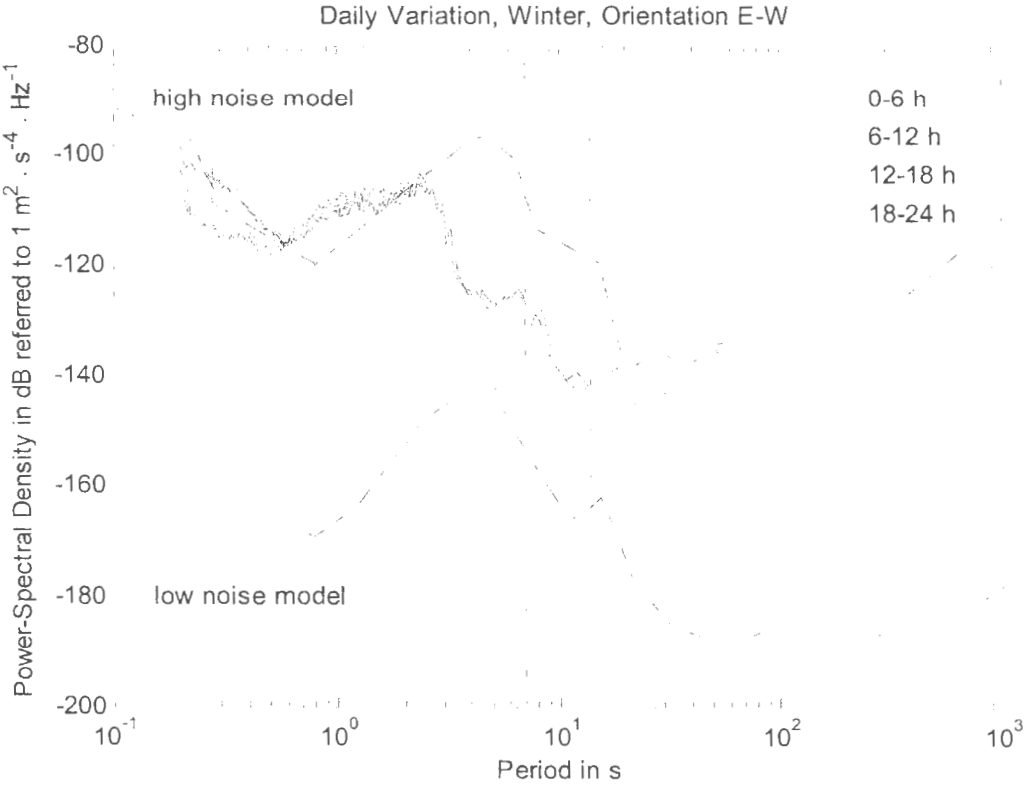


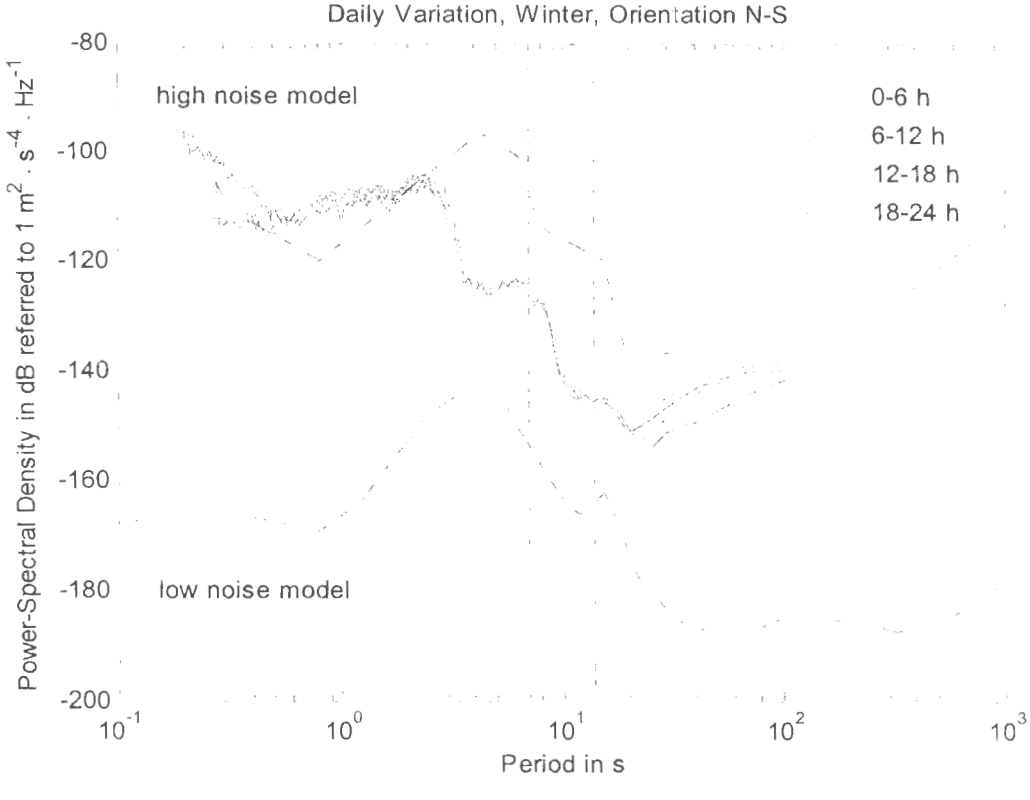

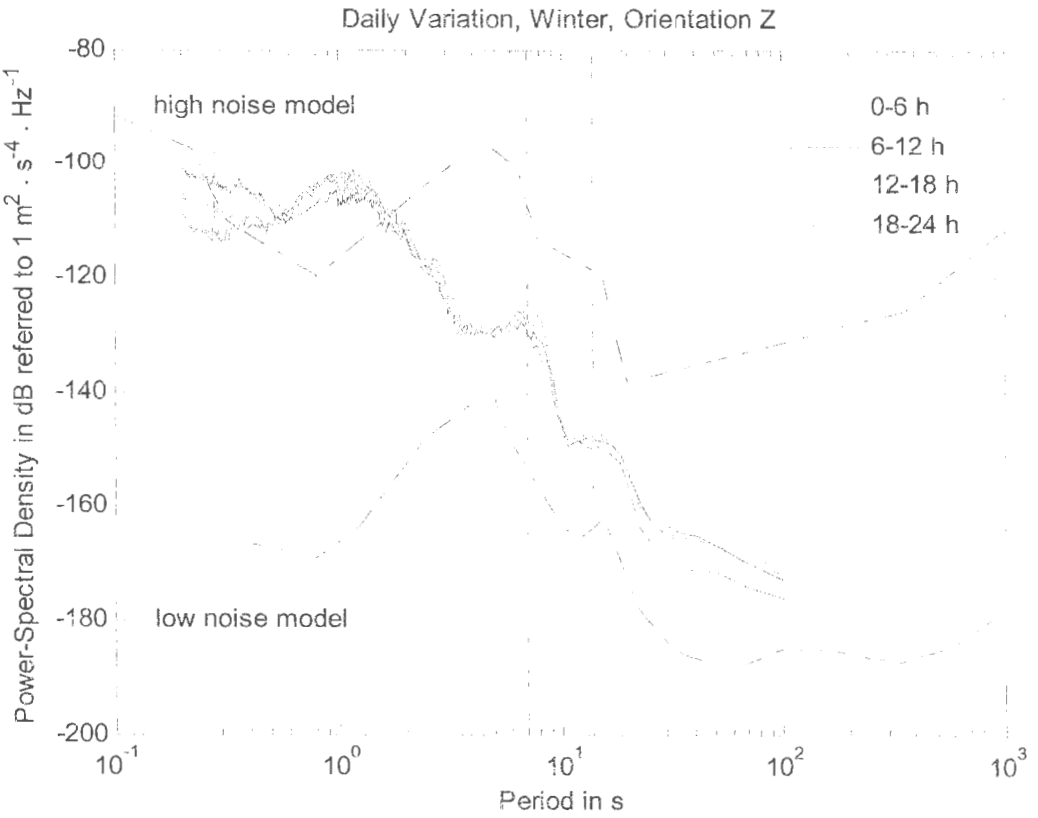
Daily Variation, Winter, Orientation Z
high noise model
low noise model
0-6 h
6-12 h
12-18 h
18-24 h
Power-Spectral Density in dB referred to 1 m² . s⁻⁴ . Hz⁻¹
-80
-100
-120
-140
-160
-180
-200
10⁻¹
10⁰
10¹
10²
10³
Period in s

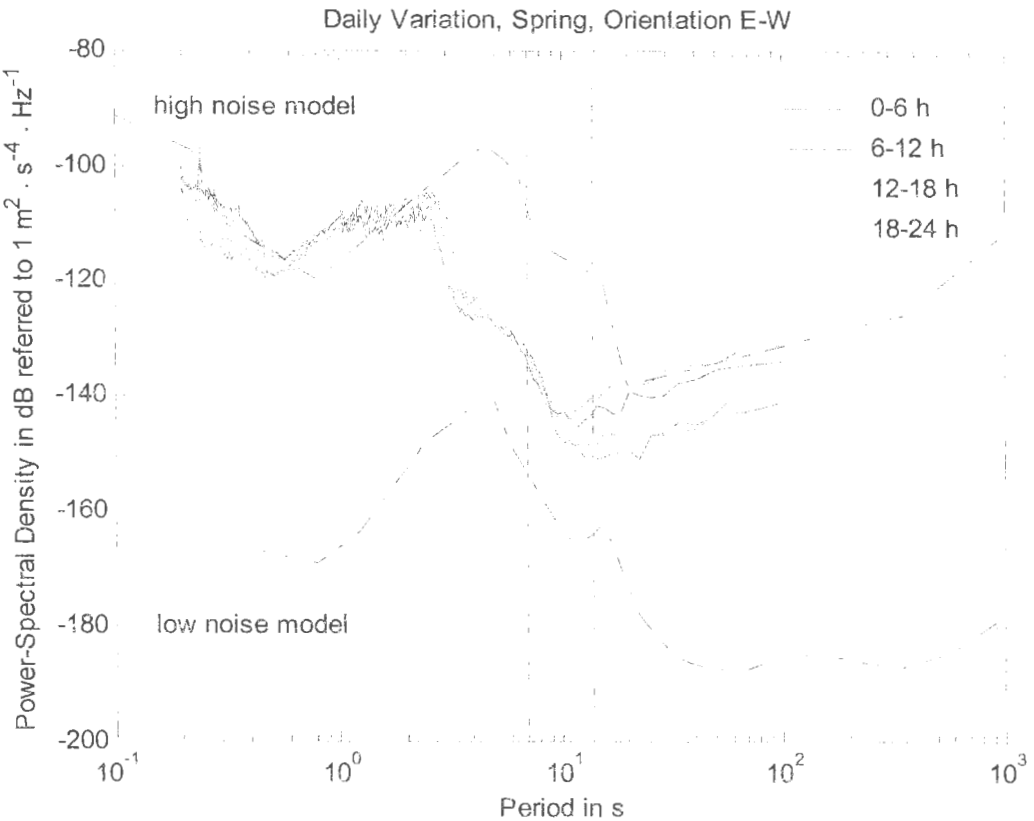
Daily Variation, Spring, Orientation E-W
high noise model
low noise model
0-6 h
6-12 h
12-18 h
18-24 h
Power-Spectral Density in dB referred to 1 m² . s⁻⁴ . Hz⁻¹
-80
-100
-120
-140
-160
-180
-200
10⁻¹
10⁰
10¹
10²
10³
Period in s

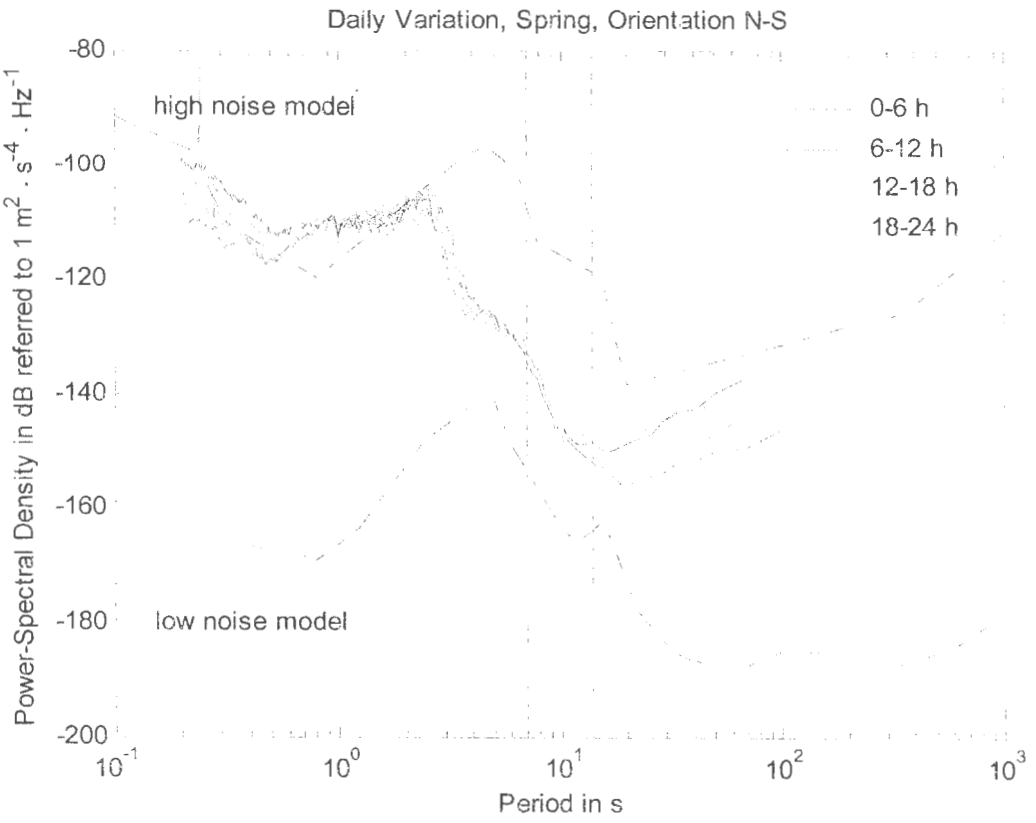
Daily Variation, Spring, Orientation N-S
high noise model
low noise model
0-6 h
6-12 h
12-18 h
18-24 h
Power-Spectral Density in dB referred to 1 m² · s⁻⁴ · Hz⁻¹
-80
-100
-120
-140
-160
-180
-200
10⁻¹
10⁰
10¹
10²
10³
Period in s

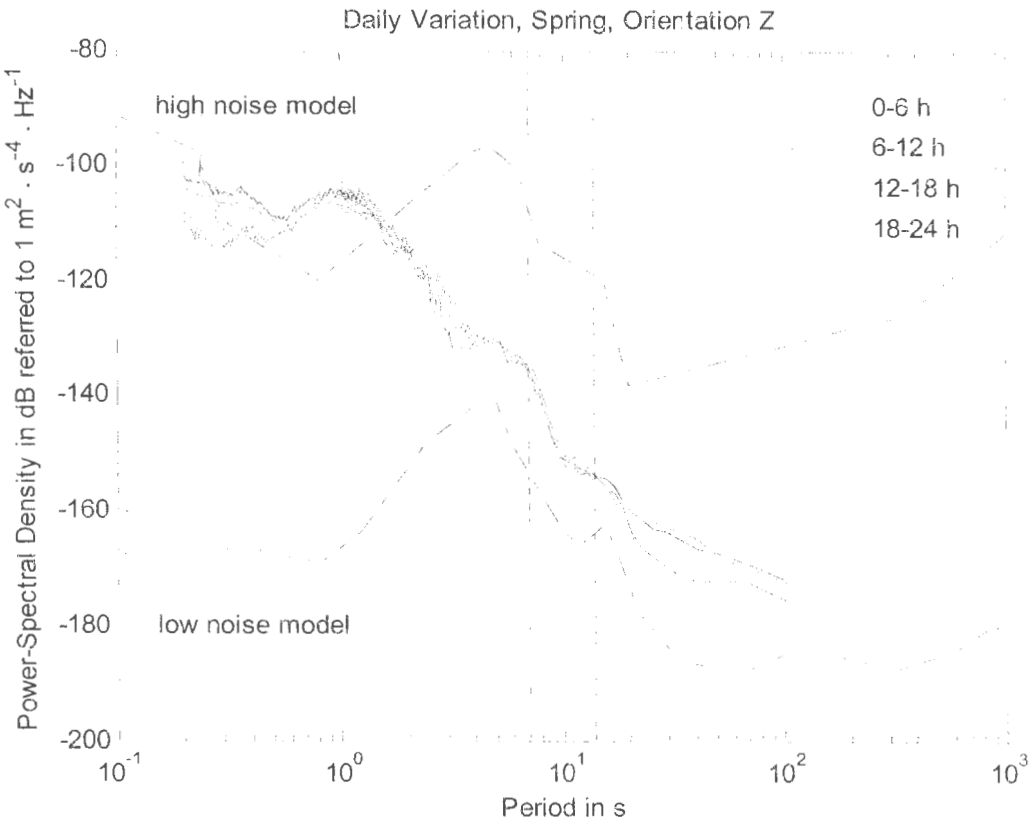
Daily Variation, Spring, Orientation Z
high noise model
low noise model
0-6 h
6-12 h
12-18 h
18-24 h
Power-Spectral Density in dB referred to 1 m² · s⁻⁴ · Hz⁻¹
-80
-100
-120
-140
-160
-180
-200
10⁻¹
10⁰
10¹
10²
10³
Period in s

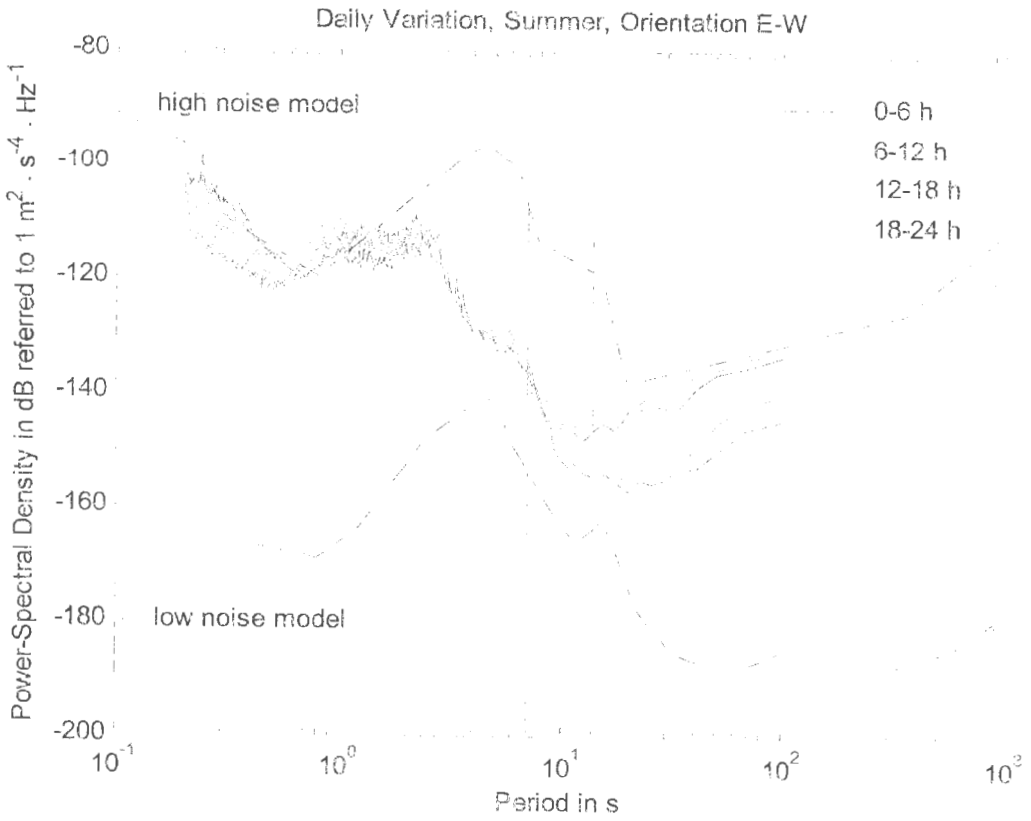
Daily Variation, Summer, Orientation E-W
-80
-100
-120
-140
-160
-180
-200
high noise model
low noise model
0-6 h
6-12 h
12-18 h
18-24 h
Power-Spectral Density in dB referred to 1 m² · s⁻⁴ · Hz⁻¹
10⁻¹
10⁰
10¹
10²
10³
Period in s

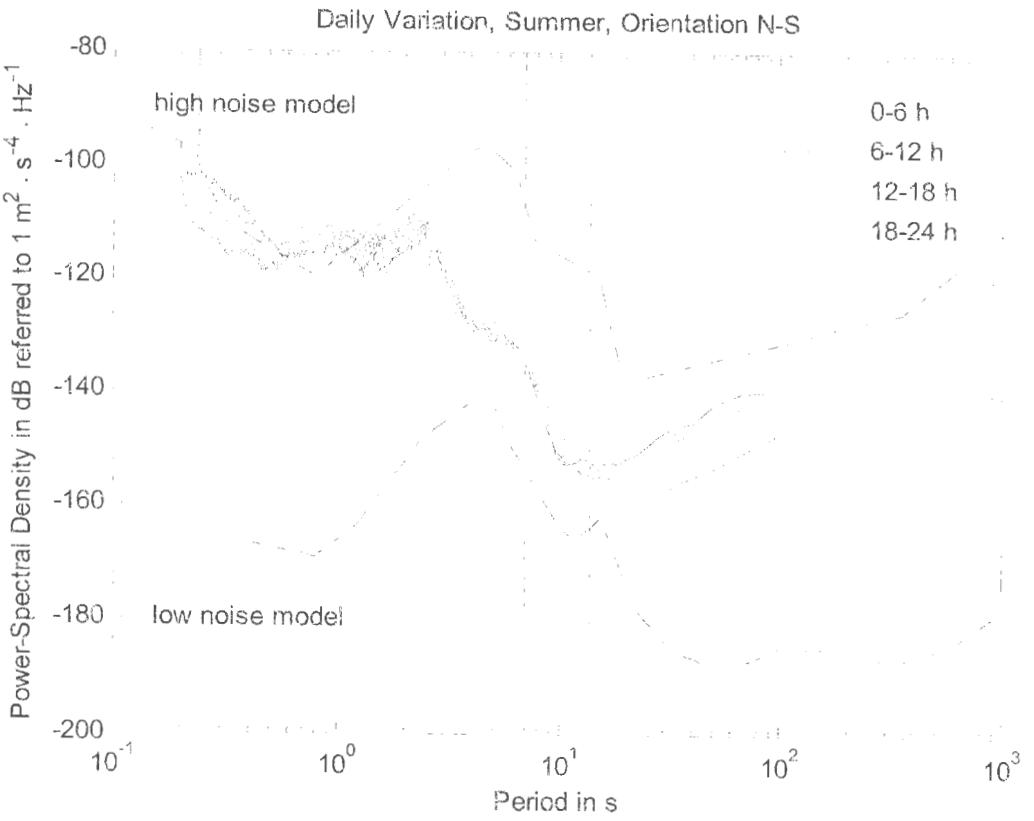
Daily Variation, Summer, Orientation N-S
-80
-100
-120
-140
-160
-180
-200
high noise model
low noise model
0-6 h
6-12 h
12-18 h
18-24 h
Power-Spectral Density in dB referred to 1 m² · s⁻⁴ · Hz⁻¹
10⁻¹
10⁰
10¹
10²
10³
Period in s

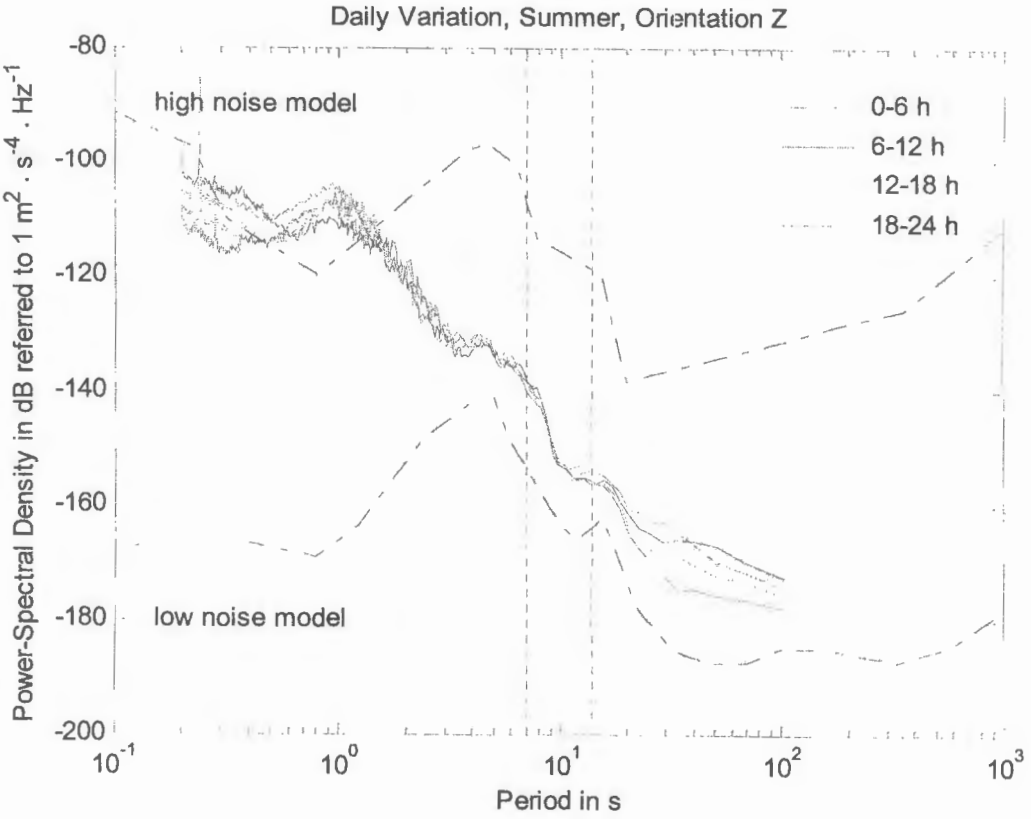
Daily Variation, Summer, Orientation Z
high noise model
low noise model
0-6 h
6-12 h
12-18 h
18-24 h
Power-Spectral Density in dB referred to 1 m² . s⁻⁴ . Hz⁻¹
-80
-100
-120
-140
-160
-180
-200
10⁻¹
10⁰
10¹
10²
10³
Period in s

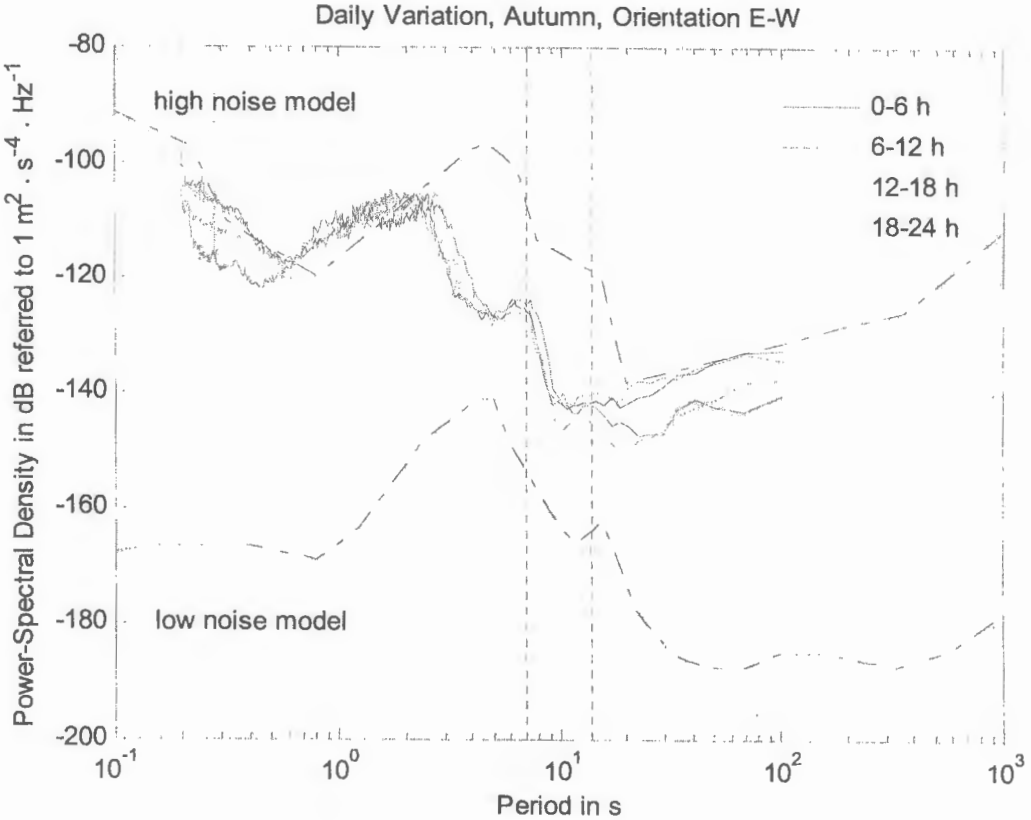
Daily Variation, Autumn, Orientation E-W
high noise model
low noise model
0-6 h
6-12 h
12-18 h
18-24 h
Power-Spectral Density in dB referred to 1 m² . s⁻⁴ . Hz⁻¹
-80
-100
-120
-140
-160
-180
-200
10⁻¹
10⁰
10¹
10²
10³
Period in s

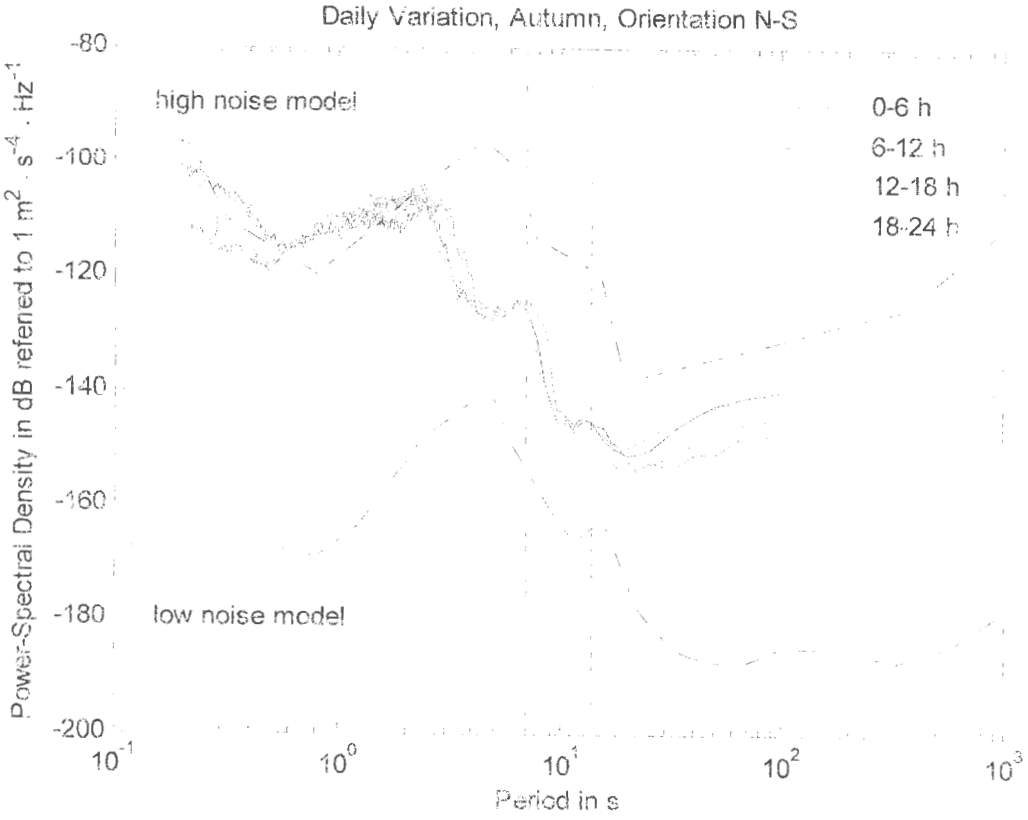
Daily Variation, Autumn, Orientation N-S
high noise model
low noise model
0-6 h
6-12 h
12-18 h
18-24 h
Power-Spectral Density in dB refered to 1 m² · s⁻⁴ · Hz⁻¹
-80
-100
-120
-140
-160
-180
-200
10⁻¹
10⁰
10¹
10²
10³
Period in s

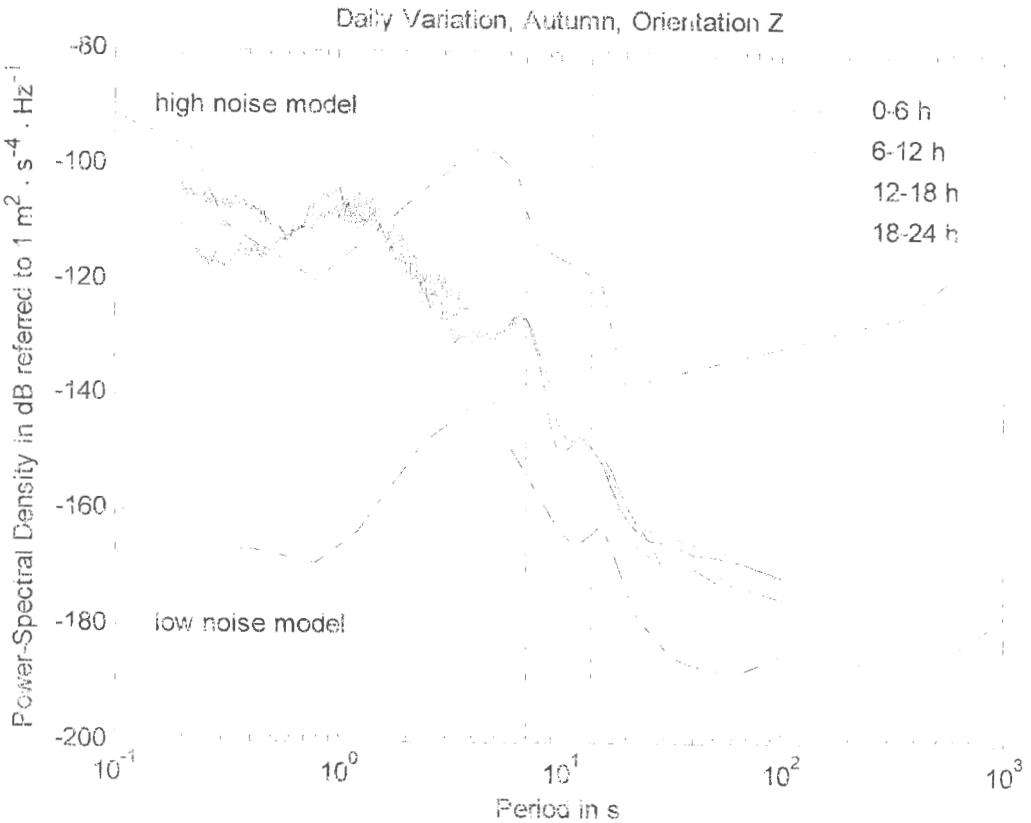
Daily Variation, Autumn, Orientation Z
high noise model
low noise model
0-6 h
6-12 h
12-18 h
18-24 h
Power-Spectral Density in dB referred to 1 m² · s⁻⁴ · Hz⁻¹
-80
-100
-120
-140
-160
-180
-200
10⁻¹
10⁰
10¹
10²
10³
Period in s

# Appendix C2

# Appendix C2 – Daily variations based on modified intervals

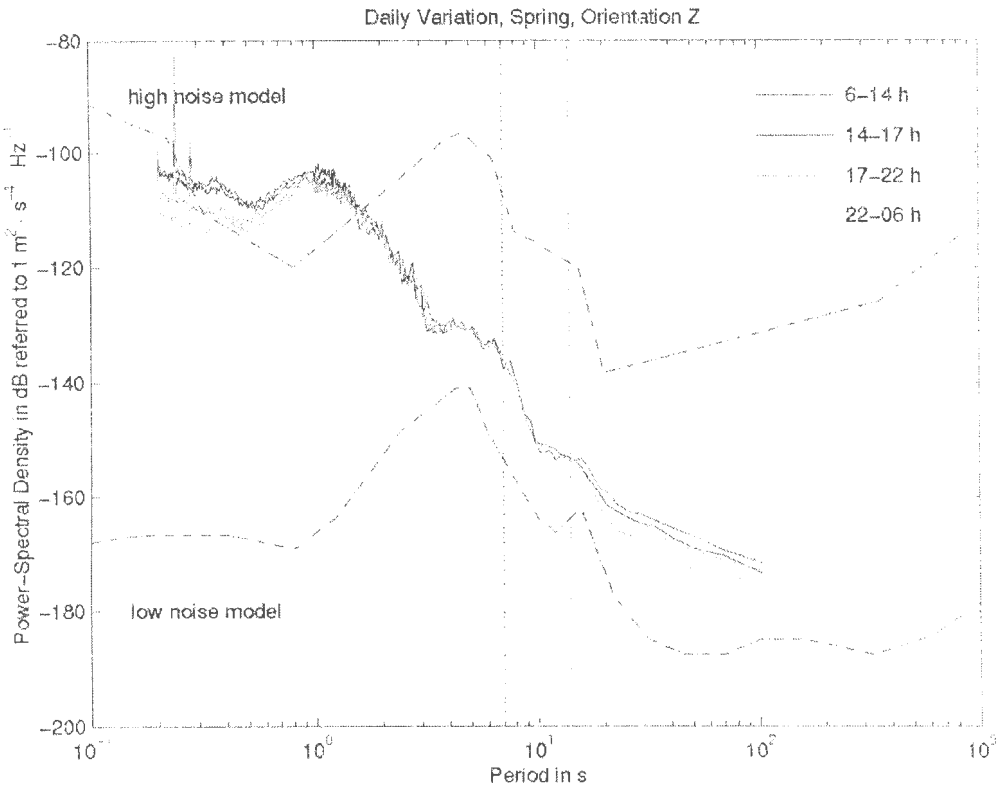

## Bibliography


AKI, K. and P. G. RICHARDS, 2002. *'Quantitative Seismology'*, University Science Books, 700 pp.

BORMANN, P., 2002. *'IASPEI New Manual of Seismological Observatory Practice (NMSOP)'*, GeoForchungsZemtrum Potsdam, Vol. 1.

BUFORN, E., A. UDÍAS, J. MARTÍN DÁVILA, W. HANKA and A. PAZOS, 2002. *'Broadband Station Network ROA/UCM/GFZ in South Spain and Northern Africa'*, Seism. Res. Letters, Vol. **73**, No. **2**, pp 173-176.

CESCA, S., 2001a. *'Estudio del ruido sísmico en la estación de banda ancha de San Fernando (SFUC)'*, Thesis, Department of Physics of the Earth, Atronomy and Astrophysics, Universidad Complutense de Madrid, 81pp.

CESCA, S., 2001b. *'Guía al análisis del ruido sísmico en estaciones de banda ancha'*, Internal Publication, Department of Physics of the Earth, Atronomy and Astrophysics, Universidad Complutense de Madrid, 18pp.

GORDEEV, E. I., V. A. SALTYKOV, V. I. SINITSIN and V. N. CHEBROV, 1992. *'Relationship between heating of the ground surface and high-frequency seismic noise'*, Phys. Earth Planet. Inter., **71**, 1-5

HANKA, W., 2002. *'Parameters which influence the very long-period performance of a seismological station: examples from the GEOFON Network'*. In: BORMANN, P. (Ed.) 2002. *'IASPEI New Manual of Seismological Observatory Practice (NMSOP)'*. GeoForchungsZemtrum Potsdam, Vol. 1, pp 64-74.

IRIS, 1993b. *'Federation of Digital Seismograph Networks Station Book'*, Incorporated Research Institutuions for Seismology (IRIS), 203 pp.

PAROLAI, S. and C. MILKEREIT, 2002., *'New relationships between $v_s$, thickness of sediments, and resonance frequency calculated by the H/V ratio of seismic noise for the Cologne area (Germany)'*, Bull. Seism. Soc. Am., **92**, 2521-2527.

PETERSON, J., 1993. *'Observation and Modelling of Seismic Background Noise'*, *USGS Open-File Report*, **93-322**, 95 pp.

PRIVALOVSKIY, N. K. and I. A. BERESNEV, 1994. *'Seismic noise emission induced by seismic waves'*, Geophys. J. Int., **166**, pp. 806-812

ROA, 2001. *'Anales 2001 – Observaciones Meteorlógicas, Sísmicas y Geomagnéticas'*, Real Instituto y
Observatorio de la Armada, San Fernando (Cádiz), pp. 165-170.

RUBIO, A., 2001. *'Catálogo de formas de onda'*, Dpto. de Física de la Tierra, Astronomía y Astrofísica I, UCM, 216pp.

MINISTERIO
DE DEFENSA

PUBLICACIONES
Pd
DE DEFENSA